Project work

Fluid mechanical analysis of an existing radial compressor and design of an adapted single-shaft jet engine for model airplanes

By Kuckelkorn, Christoph 345004 and
Hahn, Johannes 345439

This work was presented at the
Institute for Jet Propulsion and
Turbomachinery

Faculty of Mechanical Engineering of
the
Rhenish-Westphalian Technical University Aachen

Head of Institute: Prof. Dr. Peter Jeschke
Supervisor: Dr.-Ing. Daniel Grates

Aachen, May 04, 2018

Table of contents

Formula symbol

a	Work, speed of sound, logarithmic spiral parameter
A	(cross-sectional) area
b	Width
c	Absolute speed
c_p	isobaric heat capacity
c_v	isochoric heat capacity
d	Diameter, characteristic length, profile thickness
D	Twist
e	Unit vector
E	Energy
F	Power
g	Gravitational constant
h	Height
H_u	Calorific value
I	impulse
k	Parameter logarithmic spiral
l	Length
m	Mass
M	Molar mass
n	Amount of material, speed, normal vector
p	Print
P	Performance
q	Specific heat
Q	Heat
r	Radius
R	Gas constant
R_s	Specific gas constant
R_L	Specific gas constant air
s	Profile chord length
t	Time, division
T	Temperature
u	Peripheral speed
U	Inner energy
v	specific volume,
V	Volume
w	Relative speed
x	Coordinate direction
y	Coordinate direction
z	Coordinate direction, geodetic height
Z	Number of blades

α	Absolute flow angle for turbomachinery, pitch angle
β	Relative flow angle for turbomachinery
β_{BK}	Fuel/air ratio
γ	Blade angle (metal angle)
η	dynamic viscosity, efficiency
κ	Isentropic exponent
λ	Flow resistance coefficient
μ	Angular exaggeration factor
ν	kinematic viscosity
ρ	Density
ρ_h	Enthalpy degree of reaction
σ	Normal voltage
τ	Tangential voltage
φ	Angle, throughput characteristic
ϕ	Potential
ψ_h	Enthalpy parameter
ω	Angular velocity

1. Introduction

Radial compressor wheels of exhaust gas turbochargers are nowadays so well optimized and available in a wide range of sizes and variants that they are ideally suited work as compressors in a very small single-shaft jet engine. As a non-commercial project, such an engine was developed alongside my studies, but this was largely experimental. The aim is therefore to design an engine in the basic dimensions based on an existing radial compressor impeller. The basic principles are derived from the specialization courses. Now the theoretical knowledge is to be applied in practice as part of this project work. The calculations are based on thermodynamic and fluid mechanical equations. Special focus is placed on the compressor, diffuser and the turbine stage consisting of guide vane and impeller. The combustion chamber is only designed for the fuel requirement and not for geometric parameters, as this has already been developed in advance and works well.

2. Basics

This section explains the theoretical principles and design of a single-shaft jet engine as well as the thermodynamic and fluid mechanical principles on which the subsequent calculations are based.

2.1. Functionality and design Single-shaft jet engine

The important, flow-guiding components of a single-shaft jet engine are *Inlet*, *compressor*, *combustion chamber*, *turbine*, possibly an *afterburner* and the *thrust nozzle*.

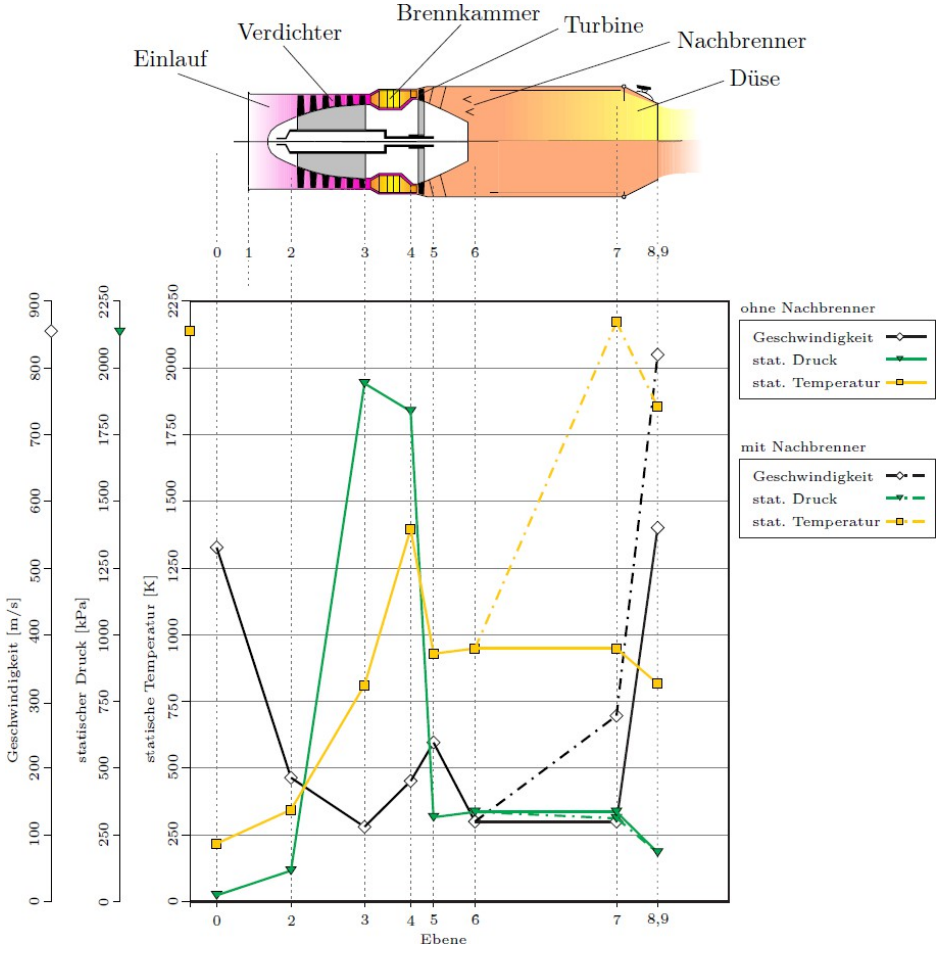

Fig. 2.1 Planes of an engine and progression of state variables during flight [Jeschke 2017b].

Based on these components, the thermodynamic states are divided into 10 states or levels according to the aeronautical manual. These are illustrated in Figure 2.1. The *inlet* has different functions depending on the operating state. In the stationary or static state, the air is drawn in from the environment and accelerated. The total temperature and the total pressure correspond to the ambient temperature and the ambient pressure. In this case, the flow velocity increases and the static pressure and temperature drop. In the case of flight at high speeds, the air is decelerated. Static temperature and static pressure increase, which is why the *inlet* in this operating state is also called *the inlet diffuser*.

The primary task of the *compressor* is to increase the pressure, as an increase in pressure is absolutely necessary so that useful work can be obtained from the thermodynamic process. This can be clearly seen in the spread of the isobars in an h-s diagram. The temperature also increases due to friction and changes in pressure and density. In principle, radial or axial compressors can be used. Radial compressors are generally used in smaller engines, as they can achieve a higher pressure ratio per stage than an axial compressor stage. Axial compressors are usually used in large engines as they are more efficient.

The task of the *combustion chamber* is to feed the chemical energy of the fuel into the fluid as efficiently as possible. The specific volume and temperature of the gas increase. For this purpose, the fuel is injected and burnt together with part of the air in the primary zone. In the secondary zone of the combustion chamber, a further air mass flow is mixed with the hot exhaust gas so that the temperature of the gas is below the maximum temperature of the turbine stages.

This gas is then expanded in the *turbine*. The static temperature and pressure drop, while the speed increases even further. The power that the turbine draws from the flow is fed to the compressor via the common shaft.

Engines that do not necessarily have to be very efficient but are intended to achieve high thrust, such as in military applications, often have an *afterburner*. Fuel is fed into this once again and burned. This increases the enthalpy as well as the static temperature and thus also the volume flow or velocity of the gas.

A further increase in speed is achieved in the *thrust nozzle*. The increase in speed is accompanied by a reduction in the static temperature and pressure, as no work is added to the fluid and the total temperature remains constant.

2.2. Thermodynamic State variables

In addition to the familiar classic state variables such as temperature T , pressure p and density ,ρ which describe the static state variables, the total state variables, such as total temperature and total pressure, are also of great importance in engine design.

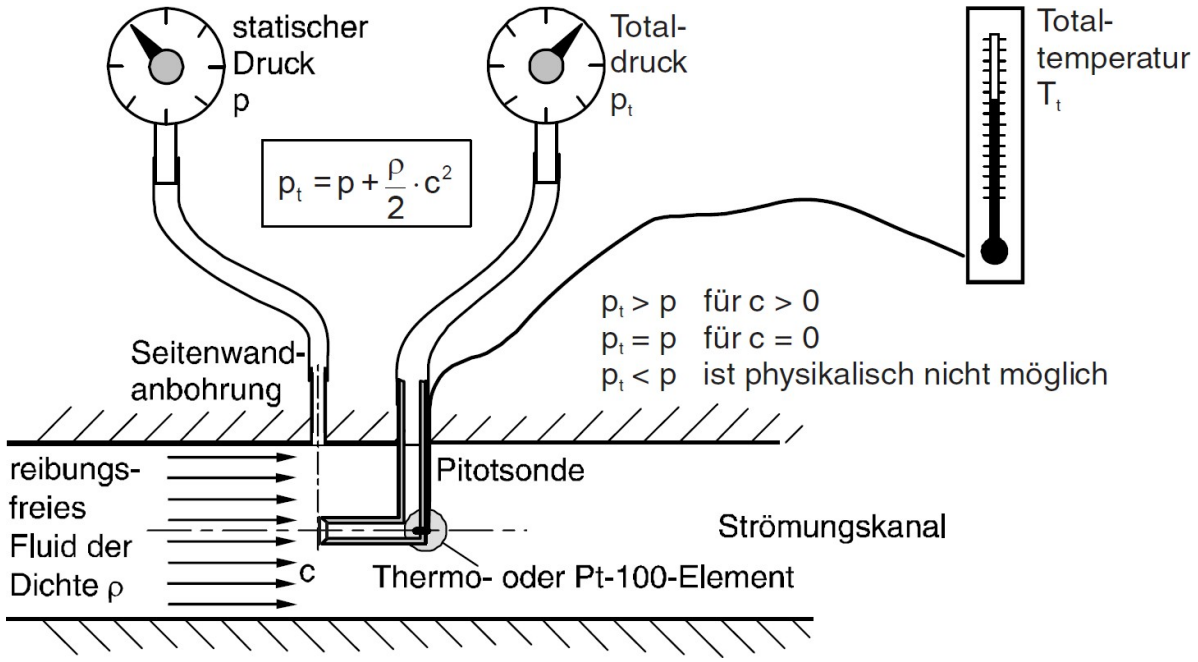

Fig. 2.2 Schematic representation of total pressure and temperature in the incompressible case [Bräunling 2009].

2.2.1 Printing and Total pressure

The static pressure of a fluid is the pressure p which it exerts at rest, i.e. when the flow velocity is zero. It is therefore the physical pressure of the fluid without the additional portion that is present due to the kinetic energy. This is taken into account in the total pressure. This pressure corresponds to the pressure that occurs when the flow is isentropically decelerated to the resting state. The equation for the total pressure can be clearly derived from the stationary, incompressible and frictionless Bernoulli equation:

$$p_1 + \frac{\rho_1}{(2)_1} c_1^2 + \rho z_1 g = p_1 + \frac{\rho_2}{(2)_2} c_2^2 + \rho z_2 g \qquad (2.11)$$

We neglect the geodesic components in our applications ($z_1 = z_2 = 0$). Furthermore, the velocity $c_2 = 0$ is defined, as this is a swirl-free flow, which results from the above definition:

$$p_t = p + \frac{\rho}{(2} c^2 \qquad (2.2)$$

2.2.2. Temperature and Total temperature

Analogous to the total pressure, the total temperature is also made up of a static and dynamic component and is defined by

$$T_t = T + \frac{c^2}{2c_p} \qquad (2.4)$$

Here, c_p is the specific heat capacity of the flowing fluid. It is easy to see that the static temperature corresponds to the total temperature when the flow velocity is zero.

2.2.3. Enthalpy and Entropy

The specific enthalpy h is a caloric state variable of thermodynamics that can be
cannot be measured directly. It can be calculated on the basis of the temperature and the specific heat capacity

$$= T \cdot c_p . \qquad (2.5)$$

The enthalpy thus has the unit $[\frac{J}{kg}]$. Formula (2.4) also yields the following for the Total enthalpy:

$$h_t = +^{c} \frac{h\,(2)}{2} \qquad (2.6)$$

The entropy*s* is also a thermodynamic state variable with the unit $[\frac{J}{K}]$.

Entropy is a measure of the disorder in a system. It increases when heat is added or through mixing (frictional losses in the flow) as well as through certain chemical reactions. In later calculations, if the isentropic efficiency of a component or the associated change of state is known, it is possible to calculate further state variables using the isentropic relationships.

2.3. Dimensionless Parameters

For the considerations of engines are usually two parameters of fluid mechanics are usually decisive. These are Mach number and Reynolds number.

The Mach number is defined by

$$Ma = \frac{c}{a} = \frac{c}{\sqrt{\kappa R_s T}} \qquad (2.7)$$

This indicates the ratio of velocity to the speed of sound. Here, κ is the isentropic exponent of the fluid and R_L is the gas constant related to the molar mass (also known as the specific gas constant).

The Reynolds number is defined by

$$Re = \frac{\rho c d}{\eta} = \frac{c d}{\nu} \qquad (2.8)$$

This indicates the ratio between inertia forces and viscosity forces. η is the dynamic viscosity. The dynamic viscosity can be converted into the kinematic viscosity ν using the density. The characteristic length d depends on the shape of the body around or through which the flow passes.

2.4. Ideal Gas law

An ideal gas is an idealized model of a real gas. In contrast to the real gas, the gas molecules are assumed to be mass points that have no intrinsic volume. The model of the ideal gas also states that the mass points move freely and in a straight line through the existing volume until they collide elastically with another particle or the wall of the volume. The ideal gas can be described by a thermal equation of state; this is referred to as the general or ideal gas equation

$$p \cdot V = m \cdot R_s \cdot T. \qquad (2.9)$$

From this equation, it can then be concluded that the product of the pressure p and the volume V is equal to the product of the specific gas constant R_s, the temperature T and the mass*m* is. The specific gas constant is calculated from the respective molar mass M_i and of the general gas constant R= 8.3144598 J mol^{-1} K^{-1} is calculated as follows,

$$R_i = \frac{R}{M_i} \qquad (2.10)$$

If, for example, the specific gas constant of air R_L is determined using the general gas constants and the molar mass for dry air M_L= 28.949 g/mol, the result is 287.1 J Kg^{-1} K^{-1}.

The specific gas constant can also be calculated from the isobaric and isochoric heat capacity calculate c_p and $c_{(v)}$:

$$R_i = cp - cv. \qquad (2.11)$$

2.5. Isentropic relationships

If a change of state is isentropic, i.e. without a change in entropy, the isentropic relationships can be used to calculate state variables. These are generally defined as:

$$\frac{p}{p_0} = \left(\frac{v_0}{v}\right)^{\kappa} \tag{2.12}$$

$$\frac{T}{T_o} = \left(\frac{v_0}{v}\right)^{\kappa-1} \tag{2.13}$$

$$\frac{T}{T_0} = \left(\frac{p}{p}\right)^{\frac{\kappa-1}{\kappa}}. \tag{2.14}$$

The isentropic exponent is defined by κ :

$$\kappa = \frac{c_p}{c_v} \tag{2.15}$$

In addition to the classic isentropic relationships, we also use the extended isentropic relationships for various calculations. These can be derived from the formula for the speed of sound and Mach number

$$a = \sqrt{\kappa R_s T}, \tag{2.16}$$

$$Ma = \frac{c}{a} \tag{2.17}$$

and the formulation of St. Venant-Wantzel

$$\frac{\kappa}{\kappa-1}\frac{p_1}{\rho_1}\left[\left(\frac{p_2}{p_1}\right)^{\frac{\kappa-1}{\kappa}} - 1\right] + \frac{c_2^2 - c_1^2}{2} = 0 \tag{2.18}$$

can be derived. We set $c_2 = 0$ and $p_2 = p_t$ and then obtain

$$\frac{p}{p_t} = \frac{1}{\left(1 + \frac{\kappa-1}{2} Ma^2\right)^{\frac{\kappa}{\kappa-1}}}. \quad (2.19)$$

The isentropic relationships give us the other equations:

$$\frac{p}{p_t} = \left(\frac{\rho}{\rho_t}\right)^{\kappa} = \left(\frac{T}{T_t}\right)^{\frac{\kappa}{\kappa-1}} \quad (2.20)$$

$$\frac{\rho}{\rho_t} = \frac{1}{\left(1 + \frac{\kappa-1}{2} Ma^2\right)^{\kappa-1}} \quad (2.21)$$

$$\frac{T}{T_t} = \frac{1}{\left(1 + \frac{\kappa-1}{2} Ma^2\right)} \quad (2.22)$$

2.6. Euler's main equation

Euler's main equation for turbomachinery is used to calculate the specific work added to or removed from the fluid. The calculated specific work is analogous to the work term of the first law of thermodynamics. Euler's main equation applies to compressible, incompressible, frictional and frictionless fluids. Euler's main equation is derived from a momentum balance of the fluid between the boundary surfaces 1 and 2 (Fig. 2.3.).

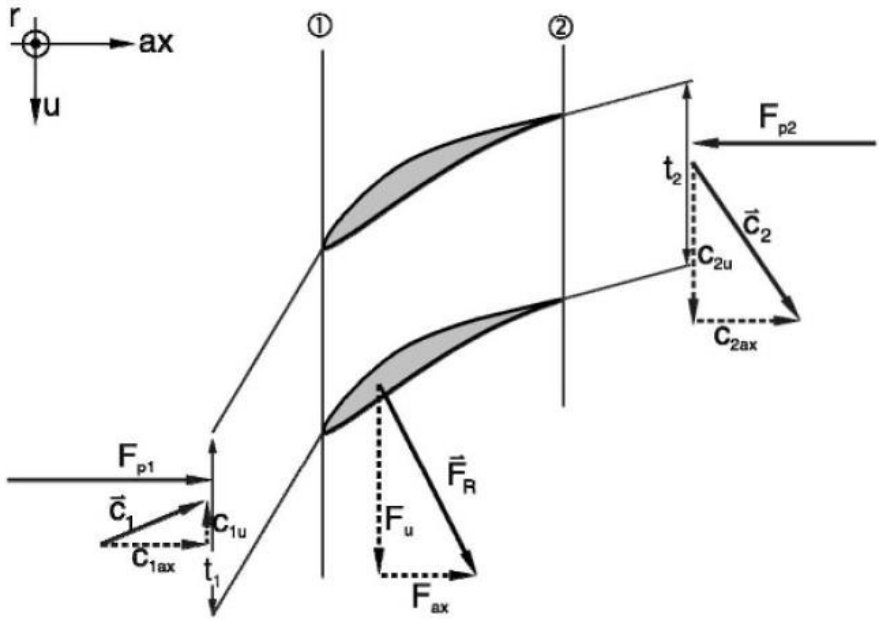

Fig. 2.3 Velocities at flow grids [Bräunling 2009].

From the law of momentum, assuming that the conservation of mass $\dot{m} = \dot{m}_{(1)} = \dot{m}_{(2)}$ applies, the following follows:

$$\vec{F}_R = \dot{m} \cdot (\vec{c}_2 - \vec{c}_1) + \vec{F}_{p2} - \vec{F}_{p1} . \qquad (2.23)$$

The resulting rotor torque can be divided into its individual components consisting of the torques on the housing M_G, hub M_N and blade M_S, but also results from the product of the radius and the momentum theorem of the circumferential direction

$$F_u = \dot{m} \cdot (c_{2u} - c_{1u}) \qquad (2.24)$$

to

$$M_{res} = r \cdot F_u = \dot{m} \cdot (r_2 c_{2u} - r_1 c_{1u}). \qquad (2.25)$$

The torques on the blade and on the hub together form the rotor torque M_R. From the Rotor power, which is expressed by the rotor torque and the angular velocity, combined with (2.25) results in

$$a_R = \frac{P_R}{\dot{m}} = \frac{M_R \cdot \omega}{\dot{m}} = \frac{(M_{res} - M_G) \cdot \omega}{\dot{m}} = (r_2 c_{2u} \omega - r_1 c_{1u} \omega) - \frac{M_G \cdot \omega}{\dot{m}}. \qquad (2.26)$$

With $u = \pi \cdot \omega$ and the assumption that the specific friction work $\frac{M_G \cdot \omega}{\dot{m}}$ is always negative and thus the specific rotor work always increases by exactly this amount and can therefore be neglected, this ultimately results in Euler's turbine equation:

$$a = u_2 c_{2u} - u_1 c_{1u}. \qquad (2.27)$$

2.7. Conservation equations

2.7.1. Law of conservation of mass

According to classical mechanics, mass is not lost and cannot be created. In order for this axiom to be implemented physically, the concept of a body is defined, which is always composed of the same mass particles. This body therefore has a fixed volume and a fixed surface area. Writing out the axiom results in

$$\frac{Dm}{Dt} = \frac{D}{Dt}\iiint \rho dV = 0. \qquad (2.28)$$

This means that the mass particles have the same mass at all times, regardless of the shape, position, volume, speed, etc. of the body.

Reynold's transport theorem states:

$$\frac{D}{Dt}\iiint \phi dV = \iiint \frac{\partial \phi}{\partial t} dV + \iint \phi c \rightarrow \cdot \vec{n} dA \qquad (2.29)$$

The left-hand term of the equation stands for the material or Lagrangian view and the right-hand side of the equation for the stationary or Eulerian view. The theorem is valid for tensors ϕ of any level.

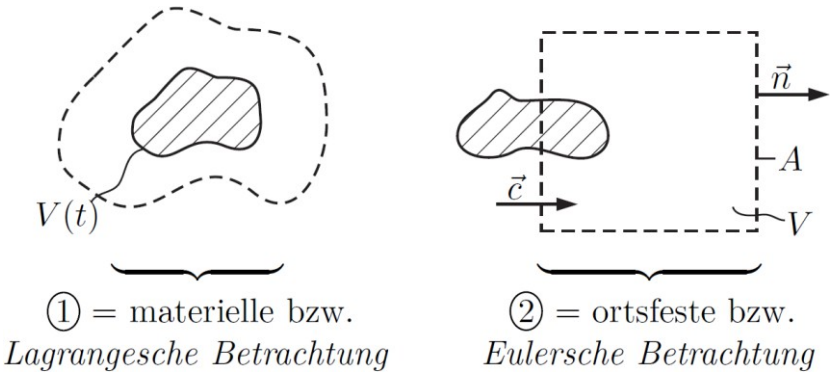

Fig. 2.4 Reynolds' transport theorem [Jeschke 2016a].

Now we set up the theorem in integral form, related to a fixed control volume in connection with Reynold's transport theorem:

$$\frac{Dm}{Dt} = \frac{D}{Dt}\iiint \rho dV = \iiint \frac{\partial \rho}{\partial t} dV + \iint \rho \vec{c} \cdot \vec{n} dA = 0 \qquad (2.30)$$

The following applies:

$\iiint \frac{\partial \rho}{\partial t} dV =$ Temporal change of mass in the system

$\iint \rho \vec{c} \cdot \vec{n} dA =$ Mass flow across the system boundary

In Fig. 2.4. it can be seen that the conservation of mass in the material volume of the moving body is equivalent to the formulation of the temporal change of mass in a fixed volume which is identical to the volume of the moving body at any given time t.

In our applications, the mass within the control volume is invariable, so this term is omitted. Only the surface integral remains. If the control volume is cleverly designed so that either a homogeneous density and velocity distribution is present, or such a distribution is approximated, the conservation of mass is achieved:

$$\sum_i \dot{m}_i = 0 \text{ with } \dot{m}_i = -\rho_i \vec{c}_i A_i \cdot \vec{n}_i \qquad (2.31)$$

2.7.2. Energy rate

The energy of a body can only change when power or heat is supplied.

$$\frac{D}{Dt}(U+E_{kin}) = P + \dot{Q} \qquad (2.32)$$

All macroscopic kinetic energies are summarized in E_{kin}. U is the sum of the internal energies, which also corresponds to the atomic kinetic energy. Furthermore, P is the power of the volume and surface forces. The amount of heat generated per unit of time is supplied to the body is referred to as $\dot{Q}$. If one applies Reynold's transport theorem to the formula results in

$$\iiint \frac{\delta}{\delta t}\left(\rho u + \rho \frac{\vec{c}\cdot\vec{c}}{2}\right) dV + \iint \left(\rho u + \rho \frac{\vec{c}\cdot\vec{c}}{2}\right) \vec{c}\cdot\vec{n}\,dA$$
$$= \iint (\bar{\bar{\sigma}}\cdot\vec{c})\cdot\vec{n}\,dA - \iint \dot{\vec{q}}\cdot\vec{n}\,dA + \iiint (\rho\vec{g}\cdot\vec{c})\,dV \qquad (2.33)$$

The following applies:

$\frac{\delta}{\delta t}\iiint \left(\left(\rho u + \rho \frac{\vec{c}\cdot\vec{c}}{2}\right)\right) dV$ = Temporal change of kinetic and internal energy in the system

$\iint \left(\rho u + \rho \frac{\vec{c}\cdot\vec{c}}{2}\right) \vec{c}\cdot\vec{n}\,dA$ = Energy flow across the system boundary

$\iint (\bar{\bar{\sigma}}\cdot\vec{c})\cdot\vec{n}\,dA$ = Power of the surface forces

$\iint \dot{\vec{q}}\cdot\vec{n}\,dA$ = Heat flow across system boundary

$\iiint (\rho\vec{g}\cdot\vec{c})\,dV$ = Power of the volume forces/gravity forces

The energy theorem is applied to a control volume where a mass flow only crosses the system boundary at "open" points. In addition, the particles in the individual mass flows should have homogeneous and identical specific properties. The result is the first law of thermodynamics

$$a+q= \quad (h_a+\frac{c_a^2}{2}+gz_a)-(h_e+\frac{c_e^2}{2}+gz_e). \qquad (2.34)$$

2.7.3. Twist set

Another conservation equation is the spin theorem. It states that the temporal change of the spin or angular momentum $\vec{D}$ is equal to the moment of the external forces

$$\frac{D\vec{D}}{Dt}=\sum \vec{M} \quad . \qquad (2.35)$$

The twist and the moments are replaced by:

$$\frac{D\vec{D}}{Dt}\iiint (\vec{x}\times(\rho\vec{c}))\ dV=\iint\vec{x}\times(\vec{\bar{\sigma}}\cdot\vec{n})\,dA+\iiint\vec{x}\times(\ )\rho\vec{g}\,dV \qquad (2.36)$$

For the left-hand side of the equation, we apply Reynolds' transport theorem and obtain

$$\iiint\frac{\delta}{\delta t}(\vec{x}\times(\rho\vec{c}))\ dV+\iint(\vec{x}\times(\rho\vec{c}))dA=\iint\vec{x}\times(\vec{\bar{\sigma}}\cdot\vec{n})\,dA+\iiint\vec{x}\times(\ )\rho\vec{g}\,dV \qquad (2.37)$$

The following applies:

$$\iiint\frac{\delta}{\delta t}(\vec{x}\times(\rho\vec{c}))\,dV=\text{Temporal swirl change in the system}$$

$$\iint(\vec{x}\times(\rho\vec{c}))dA=\text{Swirl flow across the system boundary}$$

$$\iint\vec{x}\times(\vec{\bar{\sigma}}\cdot\vec{n})dA=\text{Torque of the surface forces}$$

$$\iiint\vec{x}\times(\ )\rho\vec{g}\,dV=\text{Torque of the volume/gravity forces}$$

Now, for our application, the only volume force is gravity, which we neglect. Furthermore, we assume a stationary flow, which results in the following simplified form:

$$\iint x \rightarrow \times \rho c \rightarrow \ (c \rightarrow \bullet \vec{n} \rightarrow) dA = \iint x \rightarrow \times (\bar{\bar{\sigma}} \bullet \vec{n} \rightarrow) dA$$

(2.38) We introduce the control volume shown in Fig. 2.5. and obtain

$$M_\Omega = M_S + M_N + M_G = \dot{m} (c_{u1} r_1 - c_{u2} r_2) \qquad (2.39)$$

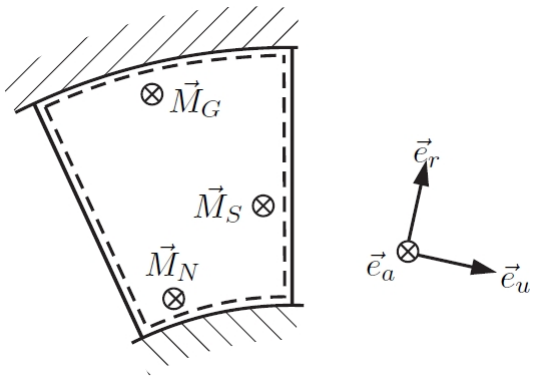

Fig. 2.5 Control volume flow passage of a guide grid [Jeschke 2016a].

M_G is the moment of the housing,M_N of the hub andM_N on the blade. Later we need the swirl theorem for an annular cross-section with flow. There, the swirl theorem is further simplified to

$$c_{u1} r_1 - c_{u2} r_2 = konst. \qquad (2.40)$$

2.7.4. Momentum theorem

In the following, the thrust equation of an engine is derived from the momentum theorem, but this can also be applied to individual components of the engine.

The change in the momentum $\vec{I}$ of a body over time is equal to the acting on the body $\vec{F}$

$$\frac{D}{Dt}\vec{I}=\vec{F} \quad . \qquad (2.41)$$

In general, this force consists of mass and surface forces. This results in

$$\frac{D}{Dt}\iiint \rho \vec{c}\, dV=\iint \bar{\bar{\sigma}}\cdot\vec{n}\, dA+\iiint \rho \vec{g}\, dV. \qquad (2.42)$$

In this formula, it has already been assumed that the only mass force acting is the force of gravity resulting from the acceleration due to gravity $\vec{g}$. The surface forces are expressed by the stress tensor $\bar{\bar{\sigma}}$. The following applies to this

$$d\vec{F}=\bar{\bar{\sigma}}\cdot\vec{n}\, dA. \qquad (2.43)$$

The stress tensor can be divided into the thermodynamic pressure p and the frictional stresses acting independently of this $\bar{\bar{\tau}}$

$$\bar{\bar{\sigma}}=-p\cdot\bar{\bar{I}}+\bar{\bar{\tau}} \quad . \qquad (2.44)$$ If the

frictional stress tensor $\bar{\bar{\tau}}$ is determined as a Newtonian fluid, the

following applies

$$\bar{\bar{\tau}}=-\frac{2}{3}\eta\nabla\cdot\vec{c}\,\bar{\bar{I}}+\eta\left(\nabla\vec{c}+(\nabla\vec{c})^{T}\right). \qquad (2.45)$$

Furthermore, the stress tensor can be converted into the stress vector using the normal vector $\vec{n}$

$$\bar{\bar{\sigma}}\cdot\vec{n}=\vec{t} \quad . \qquad (2.46)$$

The integration must always be carried out using the same moving particles. With the help of Reynold's transport theorem, the formula (2.42) can be converted into the following for a fixed control volume.

$$\iiint \frac{\delta(\rho \vec{c})}{\delta t} dV + \iint \rho \vec{c} \, (\vec{c} \cdot \vec{n}) \, dA = \iint \vec{t} \, dA \qquad (2.47)$$

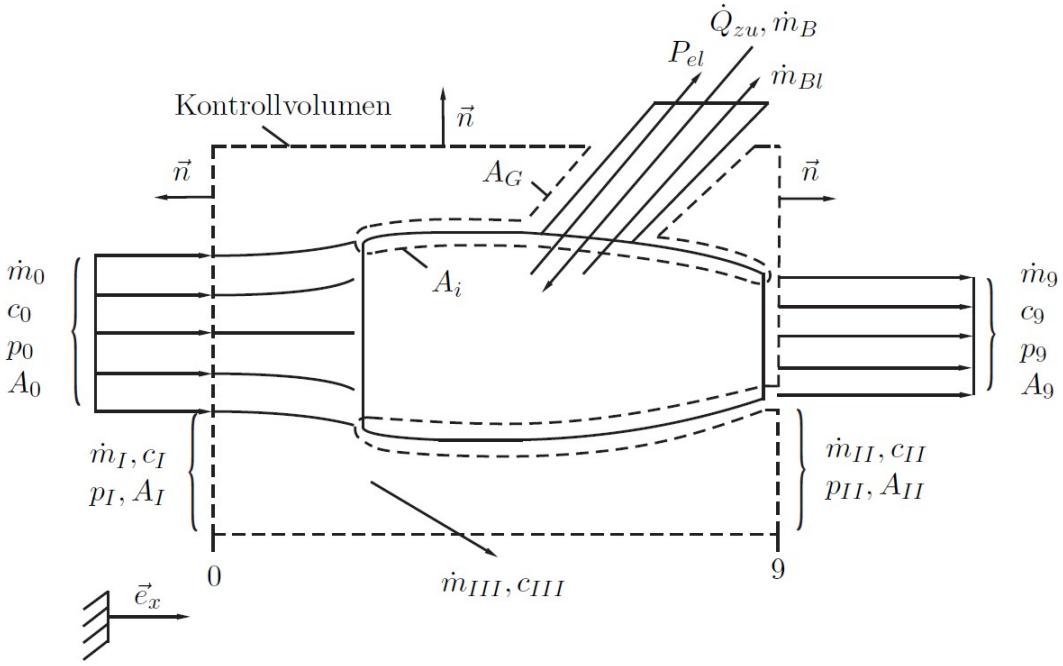

Fig. 2.6. control volume around aircraft engine [Jeschke 2017b].

The control volume was selected so that it only contains the gases flowing through, but not the metallic components of the engine. This ensures that only the force transferred from the fluid to the engine is calculated.

However, the above momentum equation only applies in this form in an inertial system without translational or rotational acceleration. Therefore, the control volume may only move at a constant speed $c_{(0)}$. This means that the stationary state of flight

or floor stand case, because the volume integrals are omitted here. The following follows

$$\iint \rho \vec{c} \, (\vec{c} \cdot \vec{n}) \, dA = \iint \vec{t} \, dA. \qquad (2.48)$$

Plane 0 is located far in front of the engine, where there is a homogeneous flow. This also applies to the side surfaces. There, the angle between the flow and the control surface is so small that its cosine is set equal to one. Furthermore, assuming homogeneous conditions in 0 and 9:

$$\vec{e}_x \cdot \iint \rho c \rightarrow (c \rightarrow \cdot \vec{n} \rightarrow) dA = \mp \dot{m} c \qquad (2.49)$$

$$\vec{e}_x \rightarrow \cdot \iint \vec{t} \rightarrow dA = \pm pA. \qquad (2.50)$$

The following applies to the momentum equation

$$-\dot{m}_0 c_o + \dot{m}_9 c_9 - \dot{m}_I c_I + \dot{m}_{II} c_{II} + \dot{m}_{III} c_{III} =$$
$$\vec{e}_x \rightarrow \cdot \iint \vec{t} \rightarrow dA_G + \vec{e}_x \rightarrow \cdot \iint \vec{t} \rightarrow dA_i + p_o A_o + p_I A_I - p_9 A_9 - p_{II} A_{II}. \qquad (2.51)$$

With

$$c_0 = c_I = c_{II} = c_{III}$$
$$p_0 = p_I = p_{II}$$
$$-\dot{m}_I + \dot{m}_{II} + \dot{m}_{III} = 0$$
$$A_9 = A_0 + A_I - A_{II}$$

follo
ws

$$F \equiv \vec{e}_x \rightarrow \cdot \iint \vec{t} \rightarrow dA_G + \vec{e}_x \rightarrow \cdot \iint \vec{t} \rightarrow dA_i = \dot{m}_9 c_9 + A_9 (p_9 - p_0) - \dot{m}_0 c_0. \qquad (2.52)$$

The thrust determined in equation (2.52) is the so-called net thrust. The gross thrust is calculated as

$$F_B = F - \dot{m}_0 c_0. \qquad (2.53)$$

Similarly, without the assumptions made above, the thrust produced by a single engine part can also be calculated using the momentum theorem. If you add up all the thrusts of the

individual components an imaginary further inflow of 0 to 1, get the net thrust again.

2.8. Speed triangles

For the modeling of a jet engine as a whole, the work conversion within the compressor and the turbine plays an important role. The work conversion in these components is closely linked with the velocity triangles . The
Velocity triangles are made up of the absolute velocity $\vec{c}$ according to the
Euler's main equation for turbines and a relative flow, which can be related as follows

$$\vec{c} = \vec{u} + \vec{w}, \qquad (2.54)$$

Converted to vector notation

$$\begin{pmatrix} c_a \\ c_u \end{pmatrix} = \begin{pmatrix} 0 \\ u \end{pmatrix} + \begin{pmatrix} w_a \\ w_u \end{pmatrix}, \qquad (2.55)$$

where u is defined as

$$u = \pi \cdot d \cdot n . \qquad (2.56)$$

The absolute and relative velocity components are made up of an axial and radial component to the meridional velocity; the respective velocity can then be determined with the aid of this and the circumferential component. The following applies

$$\vec{c}_{m1} = \vec{c}_{a1} + \vec{c}_{r1} \qquad (2.57)$$

$$\vec{c}_1 = \vec{c}_{m1} + \vec{c}_{u1}, \qquad (2.58)$$

for the velocity in the absolute system. The velocities both in state 2 and in the relative system are formulated equivalently to (2.57) and (2.58).
In order for velocity triangles to be universally understood, they are subject to certain conventions, as a result of which the circumferential components of the velocities are positive in

direction$\vec{u}$→ . Furthermore, the axial components in the exit direction must be assumed to be positive and the angles of the absolute system are described by α and in the relative system by β. In addition, the positive direction of the respective angle must be assumed to be positive in a counterclockwise direction starting from$\vec{u}$→

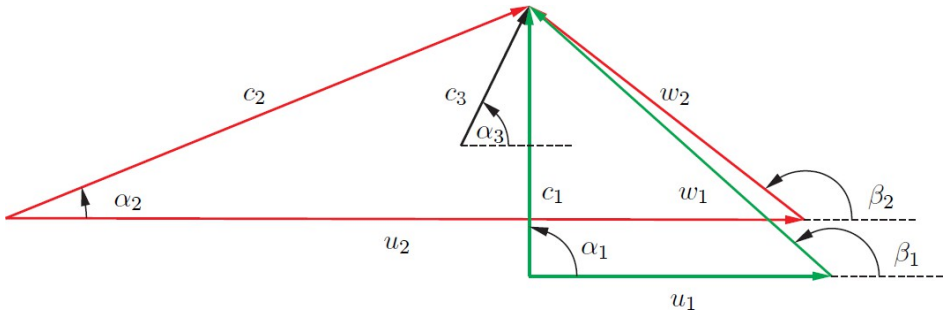

Fig. 2.7 Velocity triangle of a centrifugal compressor [Jeschke 2016a].

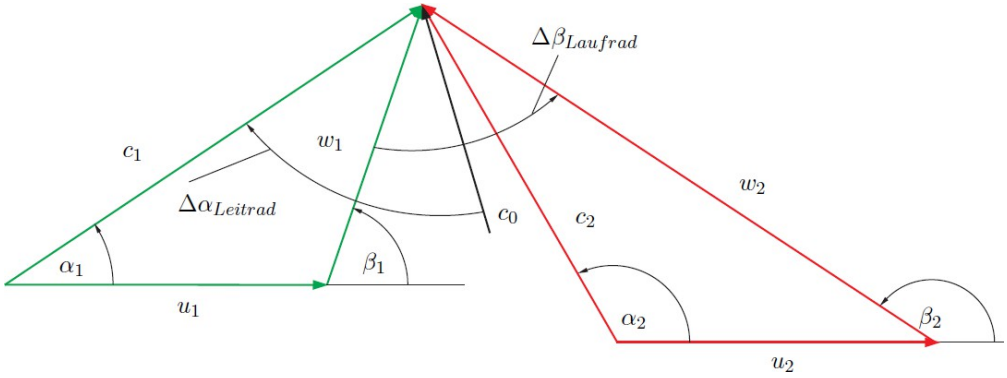

Fig. 2.8 Velocity triangle of a turbine stage [Jeschke 2016a].

2.9. Step parameters

Stage parameters are dimensionless similarity parameters that characterize the flow through a stage consisting of impeller and guide vane. Their advantage lies in the fact that they can describe the flow through the stage very well due to a small number of dependent and independent variables.

The velocity vectors within a stage are determined at three levels for compressors and turbines. Eight velocity components are sufficient in each case to determine the flow velocities. With the aid of the circumferential velocity u, these velocities are then de-dimensioned. With a impeller of a centrifugal compressor, u_2 is usually selected as the dimensioning variable, since this circumferential speed is the highest within the impeller and thus the most aerodynamically demanding conditions. With axial machines, on the other hand, the choice of circumferential speed is of little importance, as u_1 and u_2 hardly differ within a stage. each other.

The coupling of the de-dimensionalized velocities via the conservation equations with the thermodynamic state variables reduces the number of existing independent similarity variables. As the first dimensionless stage parameter, the throughput parameter is defined as follows,

$$\varphi = \frac{c_m}{u_2} \qquad (2.59)$$

This parameter is a measure of the throughput and must be determined separately at all levels if the meridional speed of the individual levels within the stage differs.

The next dimensionless step size is the enthalpy parameter

$$\Psi_h = \frac{\Delta h}{\frac{u_2^2}{2}} \qquad (2.60)$$

This is a measure of the enthalpy increase or work conversion. If the magnitude of this stage parameter increases, the relative velocities as well as the acceleration and/or the directional deflection also increase. The enthalpy value for the compressor stage is given by the formula

$$\Psi_{hV} = \frac{h_{(3)} - h_1}{\frac{u_2^2}{2}} \qquad (2.61)$$

and for the turbine stage by

$$\Psi_{hT} = \frac{h_{(2)} - h_0}{\frac{u_2^2}{2}} \qquad (2.62)$$

described.

Furthermore, we define a measure for the step division of the enthalpy increase, the so-called enthalpy reaction degree

$$\bar{h} \quad \frac{\Delta h''}{\Delta h' + \Delta h'''}. \qquad (2.63)$$

The following relationship applies to the compressor stage

$$\rho_{hV} = \frac{h_{(2)} - h_1}{h_{(3)} - h_1} \qquad (2.64)$$

and for the turbine stage

$$\rho_{hT} = \frac{h_2 - h_1}{h_{(2)} - h_0}. \qquad (2.65)$$

3. Radial compressor

3.1 Measuring the impeller

The starting point of this work is the measurement of the existing radial compressor wheel, also known as the impeller. This forms the basis for the calculations and thus also for the design of the entire engine. For some measured variables, such as angles, which can only be measured indirectly, photographs were taken of the front and side view of the impeller.

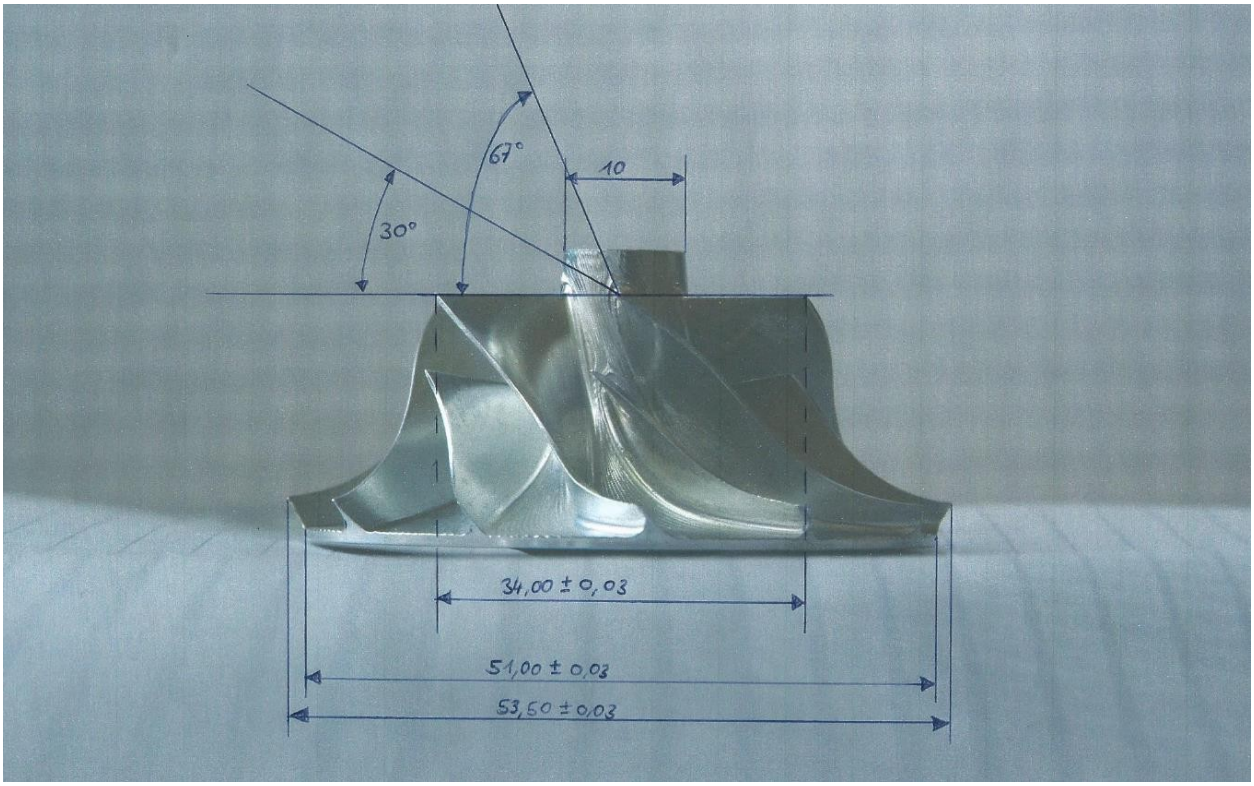

Figure 3.1. shows the following data:

	$r_1\ [mm]$	$180°-\beta_{1,s}\ [°]$	$r_2\ [mm]$
Hub	5	67	25,5
Housing	17	30	26,75

Table 3.1 Impeller measurement data

The exact metal angles at the impeller outlet are different to those at the inlet and are difficult to measure and not entirely clear in individual cases. For this reason, all blades are measured and an average value is calculated.

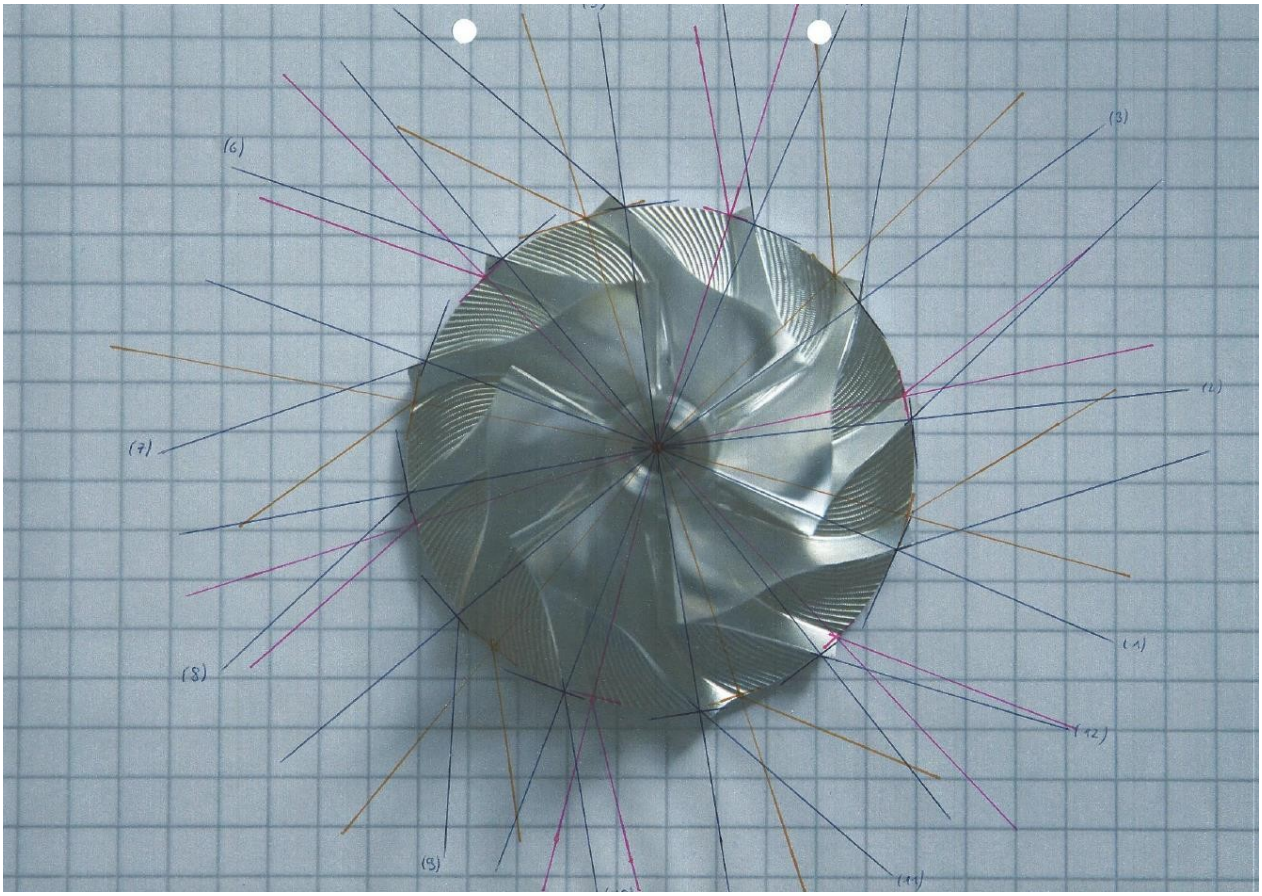

Fig. 3.2 Impeller front view with dimensions

After evaluating the angle measurements, the following averaged angle values were obtained for the outflow:

$\beta_{2,s}$ [ ] °−90°	Main Blade	Splitter Blade	Averaged
Hub	47,67	26,5	37,085
Housing	41,83	ki33	37,42
averaged	44,75	29,75	37,525

Table 3.2 Impeller measurement data

3.2. Impeller calculation

3.2.1. Calculation of mass flow & condition 1

In order to carry out the calculations, it is first necessary to know the mass flow at the design point. It is assumed that the flow angles at the housing and hub of the impeller in question are optimized. This makes it possible to set the axial velocity and thus the mass flow in such a way that there virtually no incidence angles (deviations) in the calculated flow to the existing angles. Assuming that the total pressure and total temperature in level 1 correspond to the static pressure and the static temperature of the ambient state (i.e. the inlet is adiabatic and flows through without pressure losses), the following values and data result, which are necessary for the calculation of the state variables in level 1:

$T_0 = 288,15 K$	$p_o = 101325 Pa$	$\rho_0 = 1,225\ Kg/m^3$	$\kappa = 4$
$T_{t1} = 15 K$	$p_{t1} = Pa$	$R_L = 287 Jkg^{-1}K^{-1}$	$cp = 1004.5 Jkg^{-1}K^{-1}$
$D_{1N} = 10 mm$	$D_{1G} = 34 mm$	$\beta_{1N,s} = 67°$	$\beta_{1G,s} = 30°$

Table 3.3 Output values level 1

In the following equations, the axial velocity is not yet known, but is adjusted at the end by trial and error so that the incidence angle almost disappears. The static temperature can be calculated from this and the total temperature using equation 2.4:

$$T_1 = T_{t1} - \frac{c_{m1}}{(2)\ 2cp} \qquad (3.1)$$

It is now possible to calculate the Mach number from the axial velocity and the temperature using equation 3.1:

$$Ma = \frac{c_{m1}}{\sqrt{\kappa R T_1}}. \qquad (3.2)$$

The total density is calculated using the ideal gas equation:

$$\rho_t = \frac{p_{t1}}{T_{t1} R_L}. \qquad (3.3)$$

Equation 3.3 and the extended isentropic relationships the density:

$$\rho_1 = \frac{\rho_{t1}}{(1 + \frac{\kappa-1}{2} Ma^2)^{\kappa-1}}. \qquad (3.4)$$

The mass flow can now be calculated using the conservation of mass equation 2.31.

$$\dot{m}_1 = \frac{\pi}{4} (D_{1G}^2 - D_{1N}^2) \rho c_{1m1} \qquad (3.5)$$

The circumferential speed is calculated separately for the hub and the housing:

$$u_{1N} = 2\pi r_{(1N)} \qquad (3.6)$$

$$u_{1G} = 2\pi r_{(1G)}. \qquad (3.7)$$

With the circumferential speeds is it is possible the relative velocities of the impeller inlet flow:

$$w_{1N} = \sqrt{c_{m1}^2 + u_{1N}^2} \qquad (3.8)$$

$$w_{1G} = \sqrt{c_{m1}^2 + u_{1G}^2}. \qquad (3.9)$$

This allows us to calculate the flow angles and then compare them with the steel angles of the impeller.

$$\beta_{1N} = \arcsin\left(\frac{c_{m1}}{w_{1N}}\right) \qquad (3.10)$$

$$\beta_{1G} = \arcsin\left(\frac{c_{m1}}{w_{1G}}\right) \qquad (3.11)$$

The following angular differences are now minimized by setting the axial speed $c_{(m1)}$:

$$\Delta\beta_N = \beta_{1N} - \beta_{1N,s} \qquad (3.12)$$

$$\Delta\beta_G = \beta_{1G} - \beta_{1G,s} \qquad (3.13)$$

It can be seen that with the sensible choice for the speed of

$$N = 150000 \frac{1)}{min},$$

a mass flow of

$$\dot{m_1} = 0.1425 \frac{kg}{s}$$

results. The other results can be found in Table 3.4.

c_{m1}= 156, 25 $\frac{m}{s}$	T_1=276K	Ma_1=469	m_1=1425 $\frac{kg}{s}$
ρ_{t1}=225 $\frac{kg}{m^3}$	ρ_1= 1,100 $\frac{kg}{m^3}$		
u_{1N}= 78, 5 $\frac{m}{s}$	w_{1N}= 174. $\frac{m}{s}$	β_{1N}= 63.3°	$\Delta\beta_{1N}$= 1.7°
u_{1G}=267 $\frac{m}{s}$	w_{1G}= 309. $\frac{m}{s}$	β_{1G}= 30.3°	$\Delta\beta_{1G}$= 0.3°

Table 3.4 Results of the calculations for state 1 This results in

the velocity triangle:

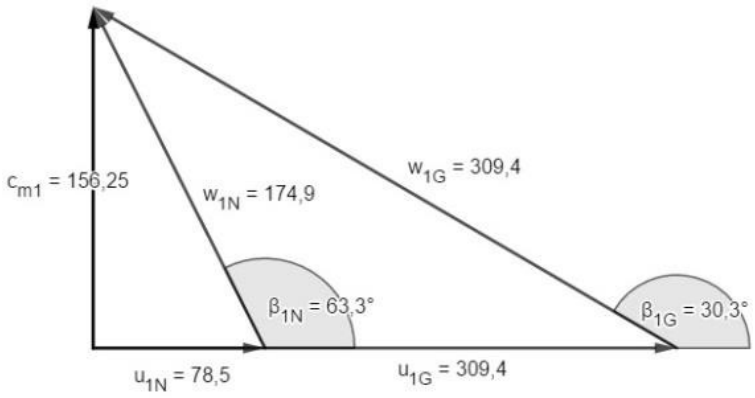

Fig. 3.3 Speed triangle in state 1

3.2.2. Calculation status 2

To be able to calculate state 2, we also need to introduce a few more values in addition to those known from state 1 (Table 3.5.). These include the number of blades ,z

Blade heightb_2 and the efficiency.

D_{2N}=51mm	z=12	η_V= 88%
β_{2s}=25°	b_2= 2.95mm	

Table 3.5 Output variables state 2

State 2 is calculated iteratively, speed and mass flow are known from state 1 and remain constant.

At the beginning, the circumferential speed is determined from the mass flow, speed and hub diameter; this is set constant over the entire iteration

$$u_2 = D_{(2N)} . \pi n \qquad (3.14)$$

Now we need to introduce a correction factorc_{slip} . This takes into account the physical phenomenon that the air does not ideally follow the blade angles during the downflow. We use an estimation according to Wiesner for the calculation:

$$c_{slip} = u_2 \sqrt{\frac{\sin(\beta_{2s})}{z^{0,7}}} . \qquad (3.15)$$

The meridional velocity$c_{(m2)}$ is as the starting value for the iteration; this is estimated with the aid of the total density, the area and the mass flow rate

$$c_{m2} = \frac{\dot{m}}{\pi D_{2N} b_2 (\rho_{Tt1RL})} . \qquad (3.16)$$

As a result this can be the circumference component of the absolute velocity can be determined from geometric relationships of the velocity triangle

$$c_{u2} = u_2 - c_{slip} - \frac{c_{m2}}{\tan(180°-\beta_{2s})}. \qquad (3.17)$$

By using Euler's main equation

$$a_v = u_2 c_{u2} - u_1 c_{u1}, \qquad (3.18)$$

whereby here

$$u_1 c_{u1} = 0 \qquad (3.19)$$

due to the swirl-free flow and the relationship from the energy theorem that

$$0 = a_V + (h_{(t1)} - h_{(t2)})$$

(3.20)

, the working conversion of the impeller can be calculated

$$_{tV} = h_{(t2)} - h_{(t1)} = u_2 c_{u2}. \qquad (3.21)$$

This allows us calculate the total temperature in state 2 by applying the following equation

$$_{tV} = h_{(t2)} - h_{(t1)} \qquad (3.22)$$

divide by c_p divide and so expressions for the total temperatureare obtained. After the total temperature by state 2, the result is

$$T = \frac{\Delta h_{tV}}{} + T \quad . \qquad (3.23)$$

Radial compressor	$t2$	c_p	$t1$	Impeller measurement

Taking into account the efficiency of the impeller, the total pressure in the state can be calculated using the isentropic relationship and the expression for calculating the total enthalpy difference

$$p_t = \left(\frac{\eta_V \cdot \Delta h_{tV}}{c_p T_{t1}}\right)^{\frac{\kappa}{\kappa-1}} p_{t1}. \qquad (3.24)$$

Now the absolute velocity must be determined, which is made up of the merdional and circumferential components using the Pythagorean theorem

$$c_2 = \sqrt{c_{m2}^2 + c_{u2}^2}. \qquad (3.25)$$

Analogous to (3.1), the static temperature in plane 2 is calculated by

$$T_2 = T_{t2} - \frac{c_2^2}{2c_p} \qquad (3.26)$$

The Mach number and the density can then be determined

$$Ma_2 = \frac{c_2}{\sqrt{\kappa R_L T_2}} \qquad (3.27)$$

$$\rho_2 = \frac{p_{(2)}}{R_L T_2} \qquad (3.28)$$

To complete the iteration, a new c_{m2} is now determined with the aid of mass conservation

$$cm2 = \frac{\dot{m}}{\rho A_2} \qquad (3.29)$$

Now (3.17)-(3.29) can be recalculated and finally the system of equations iterates against fixed values.

Table 3.6. shows the results of the calculation:

p_{t2}=208371*Pa*	p_2=143162*Pa*	T_{t2}= 363, 05*K*	T_2= 326, 13*K*
π_V=06	$_{tV}$= $\frac{J\,\Delta h}{kg}$	Ma_2= 0.752	
c_2= 272, 34 $\frac{m}{s}$	c_{m2}= 197. $\frac{m}{s}$	c_{u2}= 187. $\frac{m}{s}$	u_2= 400. $\frac{m}{s}$
w_2= 286, 98 $\frac{m}{s}$	α_2= 46.39°	β_2= 137°	

Table 3.6 Calculation parameters state 2

This results in the following speed triangle:

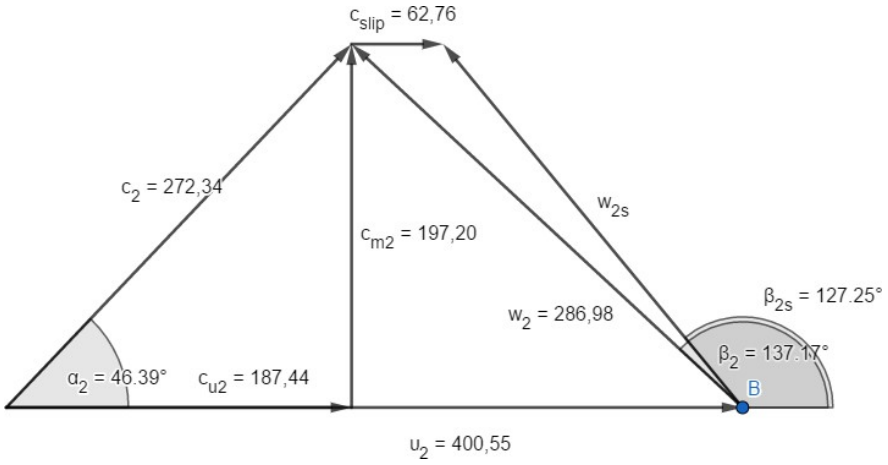

Fig. 3.4 Speed triangle in state 2

4. Diffuser

4.1 Diffuser calculation

First of all, an isentropic change of state in the diffuser is assumed for the time being. This means that

$$p_{t3,s}=p_{t2}$$
$$T_{t3,s}=T_{t2}.$$

As the pressure loss in the diffuser is to be calculated later in the chapter, it must be estimated how long the distance traveled by a fluid particle in the diffuser is. The distance traveled has the simplified form of a logarithmic spiral [Jeschke 2017c], which has the general form:

$$r(\varphi)=ae^{k\varphi} \qquad (4.1)$$

has.

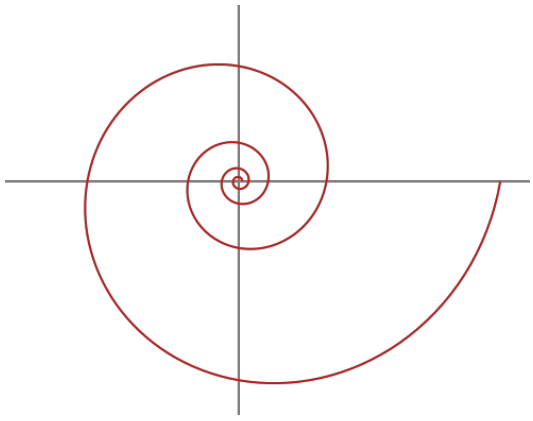

Fig. 4.1 Clockwise logarithmic spiral

In order to be able to calculate the length of the route, the parameters of equation (4.1) must first be parameterized. The parameter$k$ is the gradient of the spiral. It is calculated by:

$$k = \tan(\alpha_2). \quad (4.2)$$

Now we define a point in the polar coordinate system at which our route should start. The radius should just the radius of the compressor impeller at the outlet. The point should also lie on the Y axis.

$$r_2 = \frac{D_{2n}}{2} \quad (4.3)$$

$$\varphi_2 = \frac{\pi}{2} \quad (4.4)$$

Substitute 4.2, 4.3 and 4.4 into equation 4.1 and take the negative value of$k$, as the spiral rotates anticlockwise. Then reshape it according to the parameter$a$ and obtain

$$a = \frac{r_2}{e^{k\varphi_2}} = \frac{D_{2n}}{2 \cdot e^{-\tan(\alpha_2)\frac{\pi}{2}}}. \quad (4.5)$$

Since the diameter fixed in state 3 ($D_3 = 78mm$), we can now calculate$\varphi_{(3)}$:

$$\varphi_3 = -\ln\frac{\left(\frac{D_3}{2a}\right)}{\tan(\alpha_2)}. \quad (4.6)$$

The arc length of the distance traveled is determined as follows:

$$l = s(r_1) - s(r_2) = \sqrt{1 + k^2} \cdot \frac{r_1 - r_2}{k} = \frac{r_1 - r_2}{\sin(\alpha)} \quad (4.7)$$

This results in the following values:

k=456	a=052
φ_3= 0, 64rad=67°	l= 33mm

Table 4.1 Calculation data for logarithmic spiral

Figure 4.2. shows the logarithmic spiral plotted forφ between 0 and :$\frac{\pi}{2}$

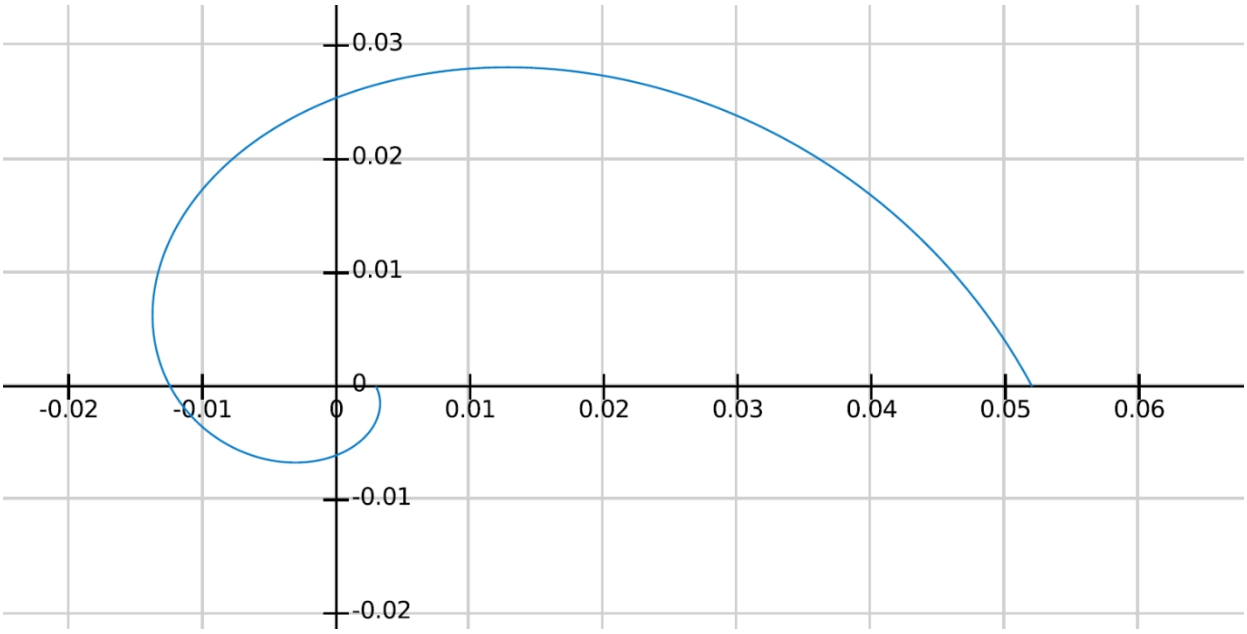

Fig. 4.2 Logarithmic spiral parameterized

Thus, the state variables and the pressure loss in the diffuser can be calculated. From the swirl equation (2.40) it follows directly for the circumferential component of the velocity:

$$c_{u3} = c_{u2} \frac{r_2}{r_3}. \qquad (4.8)$$

The angle of inclination is constant ($\alpha_{(2)} = \alpha_3$), as the side walls of the diffuser are parallel and have the same distance ($b2 = b3$). From this follows:

$$c_{m3} = c_{u3} \cdot \tan(\alpha_2), \qquad (4.9)$$

and:

$$c_3 = \sqrt{c_{u3}^2 + c_{m3}^2} \qquad (4.10)$$

The speed is used to calculate an isentropic static temperature from the isentropic total temperature:

$$T_{3,s} = T_{t3,s} - \frac{c_{t3}^2}{2c_p}. \qquad (4.11)$$

Furthermore, a Mach number can be determined which would prevail in state 3 with an isentropic change of state.

$$Ma_{3s} = \frac{c_3}{\sqrt{\kappa R T_{3s}}} \qquad (4.12)$$

In addition, an isentropic total density can be determined from the isentropic values for total pressure and total temperature:

$$\rho_{3t,s} = \frac{p_{t3,s}}{R T_{t3,s}}. \qquad (4.13)$$

The Mach number used to convert this back into a static density:

$$\rho_{3s} = \frac{\rho_{3t,s}}{\left(1 + \frac{\kappa-1}{2} Ma_{3s}^2\right)^{\kappa-1}} \qquad (4.14)$$

This results in a static pressure, which would occur after an isentropic change of state:

$$p_{3,s} = R T_{3,s} \rho_{3,s}. \qquad (4.15)$$

As the cross-section of the diffuser through which the flow passes expands and can be approximated as an unrolled square, the values such as the cross-sectional area, wetted surface, hydraulic diameter and Reynolds number are averaged.

$$A_{mittel} = b_2 \pi \frac{D_{2N} + D_3}{2} \quad (4.16)$$

$$U_{benetzt,mittell} = 2_{b(2)} + 2 \frac{D_{2N} + D_{\cdot}}{2} \quad (4.17)$$

$$D_{hydr,mittel} = 4 \frac{Amittell}{U_{benetzt,mittell}} \quad (4.18)$$

The kinematic viscosity can be regarded as an approximation constant over the change of state from 2 to 3 and is determined with the following value:

$$\nu_{mittel} = 0{,}00001 \frac{m^2}{s}.$$

The averaged Reynolds number therefore follows:

$$Re_{mittel} = \frac{c_3 \cdot D_{hy}}{{}_{,drmittel} \quad \nu_{mittel}} \quad (4.19)$$

Since we have to correct the pressure loss coefficient with a correction factor for non-circular cross-sections, we first determine the ratio of the height and width of our unrolled approximated quadrilateral.

In our case, $\frac{h_{mittel}}{b} = 0.0146$ applies, so that a correction factor of

$k_2 = 1.5$.

We use Nikuradze's approximation formula ($Re > 10^5$). This determines the pressure loss coefficient:

$$\lambda = k_2 (0.0032 + 0.221^{Re(-0.237))}_{mittel} \quad (4.20)$$

This immediately results in a pressure loss in the pipe:

$$\Delta p_{verlust} = \frac{\rho_3}{(2)\,3} c^2 \cdot \lambda \frac{l}{D_{hydr,mittel}} \qquad (4.21)$$

Subtracting the pressure loss from the isentropic static pressure in state 3 gives the correct pressure:

$$p_3 = p_{3,s} - \Delta p_{verlust} \qquad (4.22)$$

Thus, from the definition of the total pressure and the good approximation that the density in the isentropic state corresponds to the real ($\rho_3 \approx \rho_{3,s}$), the total pressure in state 3 also follows:

$$p_{t3} = p + \frac{\rho_3}{(2)\,3} c^2. \qquad (4.23)$$

Now that the static and total pressure is known, it is also possible to calculate the Mach number using the extended isentropic relationship (2.19).

$$Ma_3 = \sqrt{\frac{2}{\kappa-1}\left(1 - \left(\frac{p_3}{p_{t3}}\right)^{\frac{\kappa-1}{\kappa}}\right)\frac{1}{\left(\frac{p}{p_{t3}}\right)^{\frac{\kappa-1}{\kappa}}}}. \qquad (4.24)$$

If the equation of the total temperature (2.4) is inserted into the isentropic relationship (2.14) and transformed according to the total temperature, a determining equation is obtained for this:

$$T_{t3} = \frac{c_3^2}{2c_p\left(1-\left(\frac{p}{p_{t3}}\right)^{\frac{\kappa-1}{\kappa}}\right)}. \qquad (4.25)$$

It follows:

$$T_3 = T_{t3} - \frac{c^2}{2c_p} \qquad (4.26)$$

The calculation results in the following data:

$c_{u3} = 122,81 \frac{m}{s}$	$c_{m3} = 128,94 \frac{m}{s}$	$c_3 = 178,07 \frac{m}{s}$	$Ma_{3,s} = 477$
$\rho_{t3} = 2,0 \frac{kg}{m^3}$	$\rho_3 = 1.789 \frac{kg}{m^3}$	$\nu_3 = 0. \frac{m^2}{s}$	$Re_{mittel} = 315623$
$A_{mittel} = 00598 m^2$	$U_{benetzt,mittell} = 0,m$	$D_{hydr,mittel} = 0,0177m$	$\frac{n_{mittel}}{b} = 0.0146$
$k_2 = 5$	$\lambda = 0,0213$	$\Delta p_{verlust} = 635,Pa$	$Ma_3 = 0.490$
$p_{t3} = 209406Pa$	$p_3 = Pa$	$T_{t3} = 344.45K$	$T_3 = 328.K$

Table 4.2 Diffuser calculation variables

The conditions prevailing in state 3 are characterized by a raw friction coefficient of $\lambda = 0.0213$ and a Reynolds number of $Re = 315623$. With these values

It can be concluded from the Moody diagram that the flow in state 3 is in the turbulent region and in the transition region. This means that all the formulas we have used are applicable.

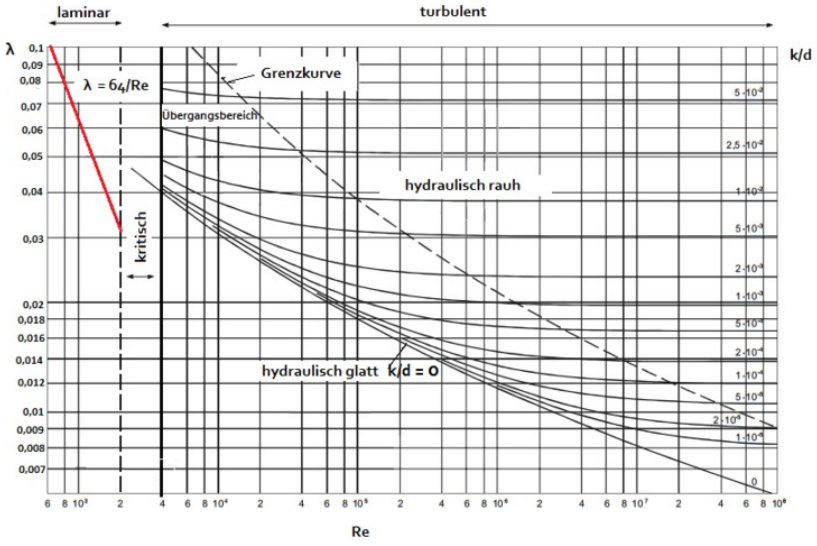

Fig. 4.3 Moody diagram [12]

5. Combustion chamber

5.1. Calculation Combustion chamber

First of all, a few assumptions must be made regarding our annular combustion chamber, which was designed and tested prior to the project work. It is assumed that the total pressure in state 4 has been reduced by five percent compared to state 3 due to losses. The static pressure, on the other hand, should be constant. Furthermore, the total temperature is set at 900 degrees Celsius.

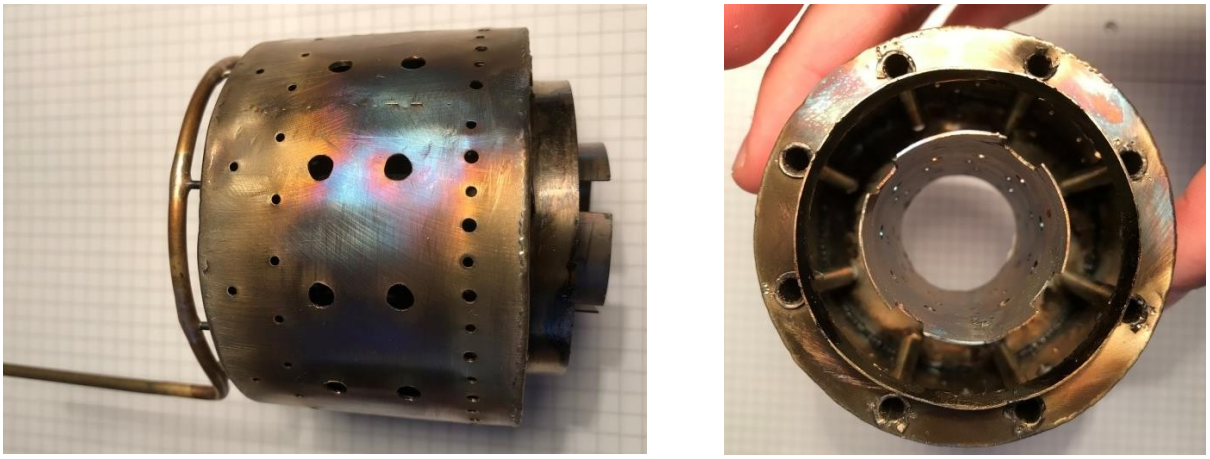

Fig. 5.1 Combustion chamber according to Kuckelkorn and Hahn

$p_{t4}=95p_{t3}=286215Pa$	$p_4=p_3=270289Pa$	$T_{t4}= 1173,16K$
$\kappa'=325$	$R'= 287 \frac{J}{kgK}$	$cp'= 1170.08 \frac{J}{kgK}$

Table 5.1 Assumptions of the combustion chamber calculation [Grates 2017].

Thus, the Mach number and the static temperature in state 4 can be calculated from the total pressure and the static pressure using the extended isentropic relationships (2.19) & (2.22):

$$Ma_4 = \sqrt{\frac{2}{\kappa-1}\left(1-\left(\frac{p_4}{p_{t4}}\right)^{\frac{\kappa-1}{\kappa}}\right)\frac{1}{\left(\frac{p}{p_{t4}}\right)^{\frac{\kappa-1}{\kappa}}}} \quad (5.1)$$

$$T_4 = \frac{T_{t4}}{1+\frac{\kappa-1}{2}Ma_4^2}. \quad (5.2)$$

From this follows directly the absolute velocity and density, which are assumed to be twist-free, which prevail in plane 4:

$$c_4 = Ma_4\sqrt{\kappa' R' T_4} \quad (5.3)$$

$$\rho_4 = \frac{p_5}{R' T_4}. \quad (5.4)$$

Furthermore, some temperature differences or expressions are calculated, which are required later in further calculations.

$$\Delta T_t = T_{t4} - T_{t3} \quad (5.5)$$

$$T_{t4} - T_o \quad (5.6)$$

$$T_{t3} - T_o \quad (5.7)$$

In addition to c_p', which only applies to air in state 4, the specific heat capacities of our fuel, butane gas, must also be determined at different temperatures. The following approximation formula is used [8]:

$$c_{p,Butan} = \frac{1000}{M_{butan}}\left(-0.05024 + 387.3\left(\frac{T}{1000}\right) - 201\left(\frac{T}{1000}\right)^2 + 40{,}64\left(\frac{T}{1000}\right)^3\right). \quad (5.8)$$

Some material values are inserted and the following data results:

$\Delta T_t = 834,3K$	$T_{t4} - T_o = 885,1K$	$T_{t3} - T_o = 64,1K$

$M_{butan} = 58,12 \frac{g}{mol}$	$M_{Luft} = 28,\frac{g}{mol}$	$H_{u,butan} = 45684\ kJ/mol$
$cp_{butan}(T_0) = 1648,2 \frac{J}{kgK}$	$cp_{butan}(T_4) = 4158.\frac{J}{kgK}$	$cp_{butan}(T_{mittel}) = 2903.\frac{J}{kgK}$

Table 5.2. material values combustion chamber

The fuel ratio of the combustion chamber is defined by

$$\beta_{BK} = \frac{\dot{m}_{Butan}}{\dot{m}_{Luft}}. \qquad (5.9)$$

Now a formula is derived to calculate the total molar mass as an expression of the fuel ratio, the molar masses of the air and the fuel. The total molar mass is defined by the expression:

$$Mges = \frac{\dot{m}_{ges}}{\dot{n}ges}. \qquad (5.10)$$

Since the total mass flow and the total mass flow can be divided into its individual components of air and butane, the expression changes to

$$Mges = \frac{mLuft+mButa}{\dot{n}Luft+\dot{n}Butan} n(.) \qquad (5.11)$$

Now the individual mass flows can be rewritten and we arrive at

$$Mges = \frac{mLuft+mButa}{\frac{mLuft}{MLuft}+\frac{mButan}{Mbutan}} n(.) \qquad (5.12)$$

Now the dimensionless fuel ratio β_{kb} can be introduced by expanding with the mass flow of the air and the expression is obtained by subsequent rearrangement

$$M_{ges} = \frac{(1+\beta_{BK})M_{luFt}}{1+\beta_{BK}(\frac{MLuFt}{MButan})}. \quad (5.13)$$

This results in the total material flow:

$$\dot{n}_{ges} = \frac{(1+\beta_{BK})\dot{m}_0}{M_{ges}}. \quad (5.14)$$

The specific heat capacity of the gas mixture of air and butane is calculated using the total mass flow rate.

$$c_{p,ges} = \frac{c_{p,Luft,mittel\,0}\dot{m}}{M_{Luft}\dot{n}_{ges}} + \frac{c_{p,Butan,mittel\,0}\beta_{BK}\dot{m}}{M_{Butan}\dot{n}_{ges}} \quad (5.15)$$

This results in a formula for calculating the combustion chamber efficiency:

$$\eta_{BK} = \frac{c_{p\beta}ges(T_{t4}-T\,0)(1+\beta)_{BK}-c_{p,}Luft(T}{\underline{t3-T\,0)}\qquad \beta_{BK}H_{u,Butan}} \quad (5.16)$$

calculate the total mass flow after the combustion chamber$\dot{m}_4$, we first determine the fuel mass flow and then the total mass flow:

$$\dot{m}_{Butan} = \beta_{BK}\dot{m}_o \quad (5.17)$$

$$\dot{m}_4 = \dot{m}_0 + \dot{m}_{Butan} \; . \quad (5.18)$$

However, as the efficiency of our combustion chamber is not known and a measurement would be very complicated, the calculations were carried out for variousβ_{BK} and listed in a table. The line from the table that had the highest efficiency was then selected.
has a realistic and conservatively estimated efficiency approx. 65% for this combustion chamber. The corresponding fuel ratio is 0.03. Table 5.3. also shows all other resulting values and parameters.

β_{BK}=03	M_{ges}= 28, 73 $\frac{g}{mol}$	$\dot{n}_{ges}$=871 $\frac{mol}{s}$	cp_{ges}=84
η_{BK}=639	$\dot{m}_{Butan}$ = 0,00324 $\frac{kg}{s}$	$\dot{m}_4$= 0. $\frac{kg}{s}$	

Table 5.3 Results of the fuel calculation

6. Turbine stage

6.1. Optimum design parameters for a turbine stage

In order to achieve the best possible work conversion, the optimum stage parameters, speeds and angles were sometimes used when designing the turbine stage. [3]

The optimum step parameters result from the derivatives set to zero

$$\frac{\partial \eta Ts,tt}{\partial \rho_h} = 0, \qquad \frac{\partial \eta Ts,tt}{\partial \varphi} = 0, \qquad \frac{\partial \eta Ts,tt}{\partial \Psi_h} = 0. \tag{6.1}$$

of the total efficiency,

$$\eta_{Ts,tt} = \Psi_h \{\Psi_h - \frac{const}{\varphi}([1-\rho_h - \frac{\Psi_h}{4}^2]+\varphi^2)^{\frac{3}{2}} \frac{const}{\varphi}([\rho_h - \frac{\Psi_h}{4}^2]+\varphi)^2\}^{\frac{3}{2}-1}. \tag{6.2}$$

This then results in the optimum stage parameters for

$$\rho = \frac{1}{2}, \qquad \varphi_{Opt} = \frac{1}{\sqrt{2}}, \qquad \Psi_{hOpt} = -2. \tag{6.3}$$

Using equation (6.3) and Figure 6.1, the two optimum angles $\beta_{1Opt} = 90°$ and $\beta_{2Opt} = 145°$ can be determined for the best possible efficiency of $\eta_s = 0.96$, but the values must be adapted for the jet turbine in question.

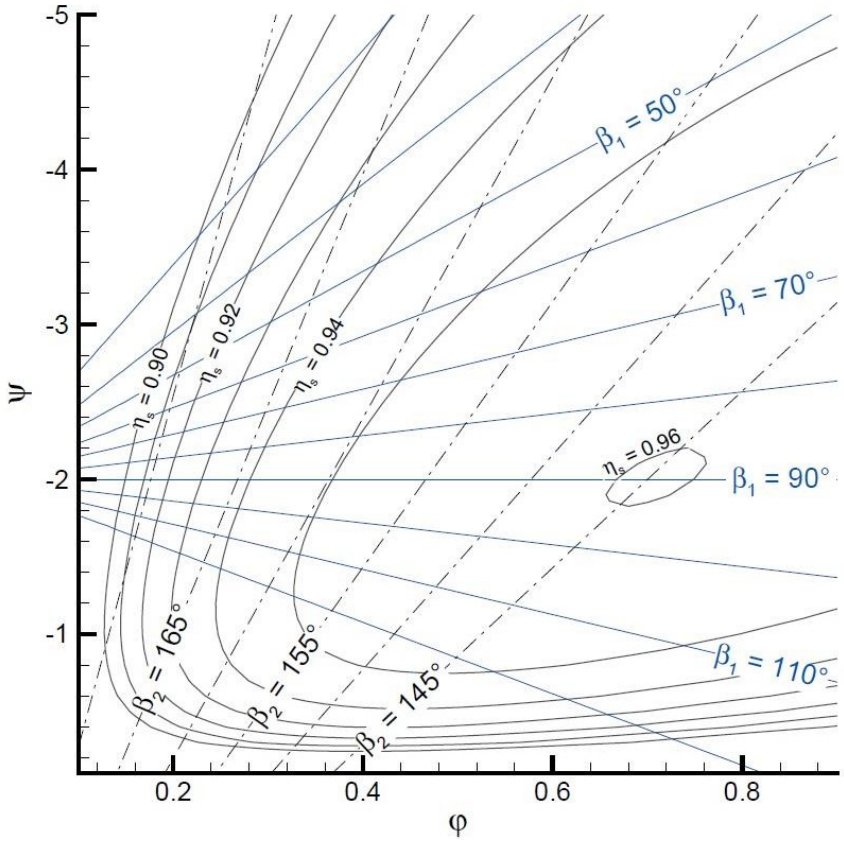

Fig. 6.1 Enthalpy parameter plotted against flow rate parameter [Jeschke 2017a].

With the help of the aero-averaging method, further relationships can be established between velocities and the step parameters, as well as between angles and the step parameters.
The following optimum speeds and angles are obtained using this method:

$$c_{1Opt} = \sqrt{\frac{3}{2}}u, \qquad c_{0Opt} = \frac{u}{\sqrt{2}}, \tag{6.4}$$

$$w_{2Opt} = \sqrt{\frac{3}{2}}u, \qquad w_{1Opt} = \frac{}{\sqrt{2}}, \tag{6.5}$$

$$\alpha_{0Opt} = 90°, \qquad \alpha_{1Opt} = \arcsin\frac{1}{\sqrt{3}} \tag{6.6}$$

$$\beta_{1Opt} = 90°, \qquad \beta_{2Opt} = \arcsin\frac{1}{\sqrt{3}} \tag{6.7}$$

6.2 Calculation of turbine inlet level: 5.0

Level 5.0 describes the state at the inlet of the stator. As this immediately follows the combustion chamber outlet, the state variables are to be equated with those from state 4 and the following applies:

$p_{(t5.}$=286215*Pa*	$p_{(5.}$=270289*Pa*	$T_{t5.0}$= 1173, 15*K*	$T_{5.0}$= 1154, 12*K*
$Ma_{5.0}$=287	$\rho_{5.0}$= 0.816 $\frac{kg}{m^3}$	$m_{5.0}$= 0. $\frac{kg}{s}$	$c_{5.0}$= 190. $\frac{m}{s}$

Table 6.1 Output variables level 5.0

We can calculate the cross-sectional area through which the flow passes directly from the values using the continuity equation.

$$A_{5.0} = \frac{\dot{m}_{5.}}{\rho_{5.0} c_{5.0}} \qquad (6.8)$$

We also set the housing radius:

$$r_{G,5.0} = 30mm.$$

We can therefore finally determine the hub radius for the stator entry plane 5.0:

$$r_{N,5.0} = \sqrt{r_{G,5.0}^2 - \frac{A_{5.0}}{\pi}}. \qquad (6.9)$$

The values for area and radius then result in:

$A_{5.0}$=000717m^2	$r_{G,5.0}$=030*m*	$r_{N,5.0}$= 0, 0269*m*

Table 6.2 Calculation variables level 5.0

6.3 Calculation turbine level: 5.1

In order to be able to calculate the state variables in level 5.1, a working equilibrium must first be established which prevails between the turbine and the compressor in the stationary operating state.

$$a_v \dot{m}_0 = -\eta_m a_t \dot{m}_5 \qquad (6.10)$$

Taking into account the law of conservation of energy, the expression (6.10) can be transformed in order to calculate the work of the turbine stage:

$$a_t = \Delta h_t = -\frac{\Delta h_{t,v} \dot{m}_0}{\eta_m \dot{m}_5}. \qquad (6.11)$$

In the following, however, the amount of work is considered. This can be used to calculate the total temperature change over the turbine stage.

$$\Delta T_{t,E} = \frac{\Delta h_t}{cp'} \qquad (6.12)$$

In addition, an efficiency of $\eta = 0.8$ is selected, as this a small turbine with relatively large gaps. From the working conversion of the turbine stage, the
Calculate total pressure ratio $\frac{p_{t2}}{p_{t0}}$

$$\frac{p_{t2}}{p_{t0}} = \eta c_p T_{t0} \left[\left(\frac{p_{t2}}{p_{t0}}^{\frac{\kappa-1}{\kappa}} - 1 \right) \right]. \qquad (6.13)$$

In addition, the loss via the impeller and guide vane can be determined, which, according to the assumption made, is divided by 50% between the above-mentioned components and can be calculated from the material model for ideal gas

$$\Delta s_{01} = c_p ln(\frac{T_{t5.1}}{T_{t5.0}}) - R_L ln(\frac{p_{t5.1}}{p_{t5.0}}) \quad (6.14)$$

$$\Delta s_{02} = c_p ln(\frac{T_{t5.2}}{T_{t5.0}}) - R_L ln(\frac{p_{t5.2}}{p_{t5.0}}) \quad (6.15)$$

However, the following applies via the stator$T_{t5.0} = T_{t5.1}$, since the entire work conversion takes place in the impeller and therefore the first term is

$$c_p ln\,(\frac{T_{t5,1}}{T_{t5.0}}) = 0. \quad (6.16)$$

This results in the following for the total pressure in state 5.1

$$p_{t5.1} = p_{t5.0} e^{-\frac{\Delta s_{01}}{R_L}}. \quad (6.17)$$

The present turbine is to have a reaction blading. In this case, the enthalpy change is divided equally between the stator and rotor. The degree of reaction therefore has the value :

$$\rho_h = \frac{\Delta h_{Rotor}}{\Delta h_t} = 0.5. \quad (6.18)$$

The following equations are also solved by iteration, but an iteration with retention of all optimal parameters leads to a geometry that cannot be produced, which is why the iteration was adjusted with the help of the angles so that a sensible turbine geometry is created. To do this, we start with the average circumferential speed. Using this, the circumferential component of the velocity can be calculated from Euler's main equation and the law of conservation of energyassuming that$c_{u5.2}$= is 0

$$c_{u5.1} = \frac{a_t}{u_{5.1}}. \qquad (6.19)$$

The speed angle can be used to further calculate

$$c_{m5.1} = \tan(\alpha_1) c_{u5.1}. \qquad (6.20)$$

The absolute speed $c_{5.1}$ is set is then from the meridional and the circumferential component using the Pythagorean theorem,

$$c_{5.1} = \sqrt{c_{m5.1}^2 + c_{u5.1}^2}. \qquad (6.21)$$

The relative angle of attack $\beta_{5.1}$ can be calculated by geometric relationships from the velocity triangle:

$$\beta_{5.1} = \pi - \arctan\left(\frac{c_{m5.1}}{u_{5.1} - c_{u5.1}}\right). \qquad (6.22)$$

The relative velocity can now be calculated using this angle and the meridional velocity of state 5.1:

$$w_{5.1} = \left(\frac{c_{m5.1}}{\sin(\pi - \beta_{5.1})}\right). \qquad (6.23)$$

The next step is to record the state variables of state 5.1 in order to be able to calculate the geometries later.
The static temperature can be calculated by rearranging equation (2.4) as the difference between the total temperature and the dynamic component:

$$T_{5.1} = T_{t5.1} - \frac{c_{5.1}^2}{2 \cdot c_p}. \qquad (6.24)$$

With the aid of the calculated temperature, the density can now be determined using the ideal gas equation and the total pressure using the isentropic relationship:

$$\rho_{5.1} = \frac{p5.}{R_{(5.1)} \cdot} \qquad (6.25)$$

and

$$pt5_{.1} = \frac{p_{5.1}}{\left(\frac{T_{5.1}}{Tt5_{.1}}\right)^{\frac{\kappa}{\kappa-1}}}. \qquad (6.26)$$

To calculate the cross-sectional area of the stator, the law of conservation of mass is due to the assumption that a homogeneous density and velocity distribution prevails in state 5. In addition, there is no mass in the transition from state

4 is supplied or discharged according to state 5, i.e. $\dot{m}_4 = \dot{m}_5$ applies. By rearranging (3.21) we obtain one

$$A5.1 = \frac{\dot{m}_4}{\rho_{5.1} \cdot cm5_{.1}}. \qquad (6.27)$$

Now that the cross-sectional area is known, the radius of the hub is derived from the geometry:

$$r_{N5.1} = \sqrt{r_G^2 - \frac{A_{5.1}}{\pi}}. \qquad (6.28)$$

Now it is possible to express the mean radius using (6.28) and the radius of the casing:

$$means = \frac{rN5.1 + rG5_{.1}}{2}. \qquad (6.29)$$

This is required to determine a new circumferential speed, which acts as the starting value in the next iteration step and from which all variables are recalculated,

$$u_{mittel} = \pi \cdot 2 \cdot r_{mittel} \cdot \frac{N}{60}. \quad (6.30)$$

finally determine all state variables, the Mach number can be calculated from the known ones:

$$Ma5_{.1} = \frac{c_{(5.1).}}{\sqrt{\kappa R T_{5.1}}} \quad (6.31)$$

Finally, the flow characteristic can be calculated

$$\varphi = \frac{c_{m5.1}}{means}. \quad (6.32)$$

We therefore calculate the following data.

$p_{(t5.}$=154984Pa	**$p_{(5.}$=172596Pa**	**$T_{5.1}$= 1142, 6K**	**$T_{t5.1}$ = 1173, 2K**
$r_{mittel5.1}$= 0, 0255m	$r_{G5.1}$= 0.03 m	$r_{N5.1}$= 0.0210 m	$_{average5.1}$ = 400.79 $\frac{m}{s}$
$c_{u5.1}$= 184, 10 $\frac{m}{s}$	$c_{m5.1}$ = 194.00 $\frac{m}{s}$	$c_{5.1}$ = 267.45 $\frac{m}{s}$	$\beta_{5.1}$= 2,411 rad
$w_{5.1}$= 290, 84 $\frac{m}{s}$	$\rho_{5.1}$= 0.5263 $\frac{kg}{m^3}$	$A_{5.1}$= 0.00144 m^2	$Ma_{5.1}$= 0.406
φ= 0.484			

Table 6.3 Results of the calculation for level 5.1

6.4 Calculation turbine level: 5.2

The size of the radius is also specified for the state after the turbine stage.

At beginning is the total temperature is calculated, one subtract the total temperature difference from the total temperature in state 5.0.

$$T_{t5.2} = T_{t5.0} - \Delta T_{t,E} \qquad (6.33)$$

It follows from the ideal angles of the speed triangles that the absolute speed in the circumferential direction is zero:

$$c_{u5.2} = 0. \qquad (6.34)$$

This means that the circumferential speed and the flow angle $\beta_{5.2}$ can be used directly to calculate the meridional velocity can be determined, which corresponds to the total absolute velocity

$$c_{m5.2} = c_{5.2} = u_{5.2} \tan(\pi - \beta_{5.2}). \qquad (6.35)$$

The other values for level 5.2 are now calculated in the same way as for turbine level 5.1:

$$w5_{.2} = \left(\frac{c_{m5.2}}{\sin(\pi - \beta_{5.2opt})}\right) \qquad (6.36)$$

$$T5_{.2} = Tt5_{.2} - \frac{c5_{.2}^2}{2 \cdot c'_p} \qquad (6.37)$$

$$\rho_{5.2} = \frac{p5_{.}}{T_{(5.2)} \cdot R} \qquad (6.38)$$

$$pt5_{.2} = \frac{p5_{.2}}{\left(\frac{T_{5.2}}{Tt5_{.2}}\right)^{\frac{\kappa}{\kappa-1}}} \qquad (6.39)$$

$$A_{5.2} = \frac{\dot{m}_{(4)}}{\rho_{5.1} \cdot cm5_{.1}} \quad (6.40)$$

$$r_{N5.2} = \sqrt{r_G^2 - \frac{A_{5.2}}{\pi}} \quad (6.41)$$

$$means = \frac{r_{N5.2} + r_{G5.2}}{2} \quad (6.42)$$

$$u_{mittel} = \pi \cdot 2 \cdot r_{mittel} \cdot \frac{N}{60} \quad (6.43)$$

$$Ma5_{.2} = \frac{c_{(5.2)}}{\sqrt{\kappa R T_{5.2}}} \quad (6.44)$$

Finallythe enthalpy parameter can be calculated

$$\Psi_{ht} = \frac{a_t}{\frac{u\_mean5.2^2}{2}} \cdot \quad (6.45)$$

The result is:

$p_{(5.} = 137624 Pa$	$p_{(t5.} = 149817 Pa$	$T_{5.2} = 1087,2 K$	$T_{t5.2} = 1110,09 K$
$r_{mitteel5.2} = 0255 m$	$r_{G5.2} = 0. m$	$r_{N5.2} = 0. m$	$u_{mittel5.2} = 400. \frac{m}{s}$
$c_{u5.2} = 0 \frac{m}{s}$	$c_{m5.2} = 213. \frac{m}{s}$	$c_{5.2} = 213, \frac{m}{s}$	$\beta_{5.2} = 2, rad$
$w_{5.2} = 462,73 \frac{m}{s}$	$\rho_{5.2} = 0.441 \frac{kg}{m^3}$	$A_{5.2} = 0.00144 m^2$	$Ma_{5.2} = 0.336$

Table 6.4 Results of the calculation for level 5.2

This results in the complete speed triangles in the turbine stage:

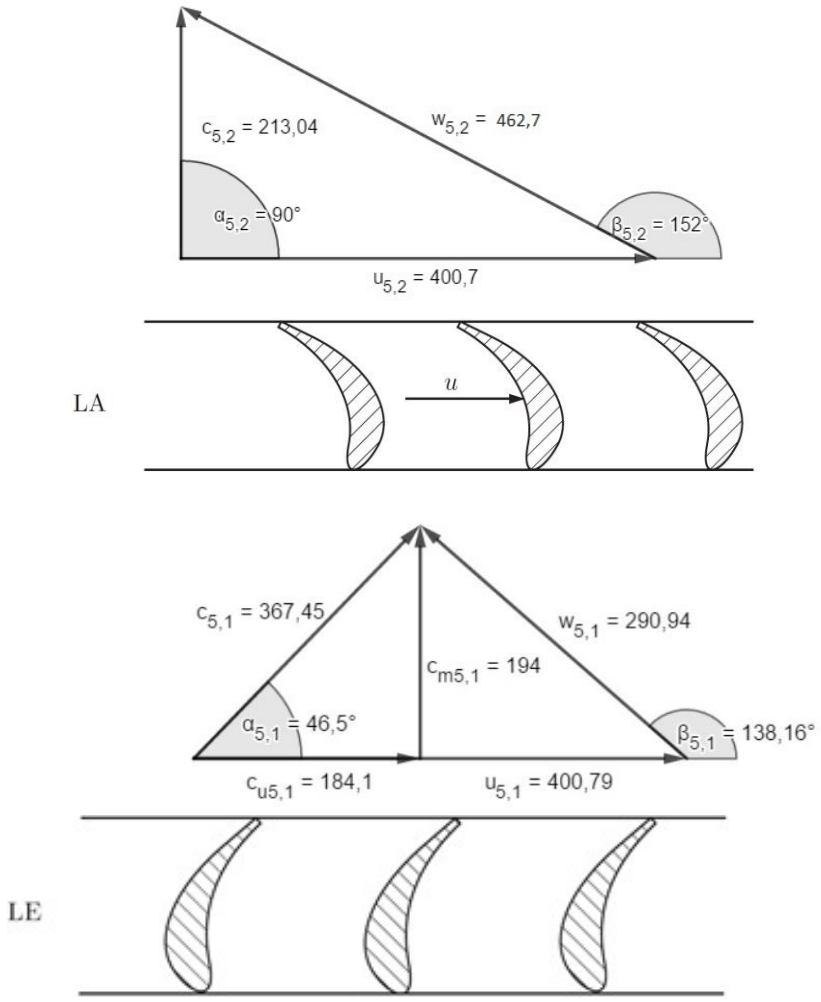

Fig. 6.2 Velocity triangles in the turbine stage

6.5 Angular exaggeration and blade geometries

Because the metal angles of the turbine stage do not exactly match the required flow angles at the leading and trailing edges, the curvature of the blade must be changed. This property describes the concept of angular misalignment. The calculation of angular displacement can be determined on the basis of potential theory.

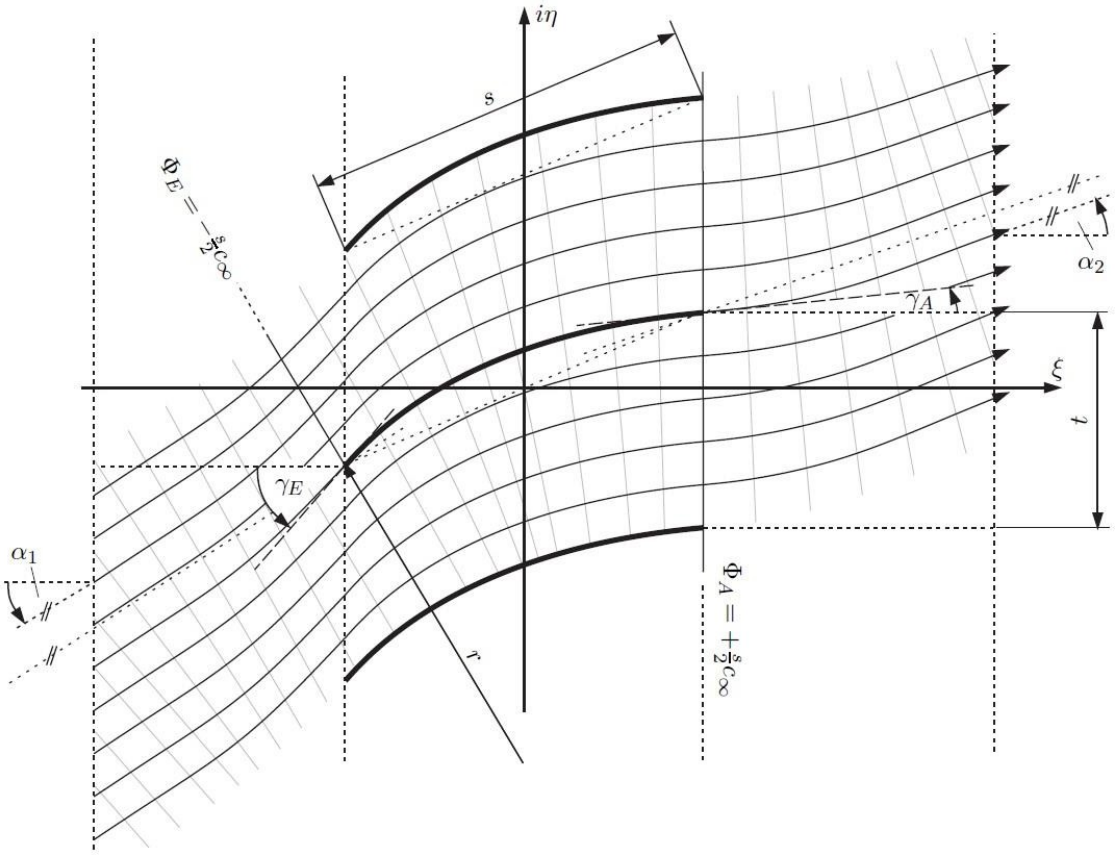

Fig. 6.3 Angular representation of the angular exaggeration (note that the indexing differs from ours) [Jeschke 2017c].

In order to be able to determine the angular overshoot of the turbine stage, a sensible and approximately optimum pitch ratio was selected in advance

$$\frac{t}{s} = 0.75 \qquad (6.46)$$

and for a high stability of the blading a thickness ratio of:

$$\frac{d_{max}}{s} = 0.1 \qquad (6.47)$$

elected.

First, the mean flow angle is calculated using the flow angles at the leading and trailing edges of the stator. This corresponds to the staggering angle in order to ensure a flow-free leading and trailing edge:

$$\alpha_m = \left(\frac{\alpha_{50}+\alpha_{51}}{2}\right) = \left(\frac{\gamma_0+\gamma_1}{2}\right) = \gamma_m \qquad (6.48)$$

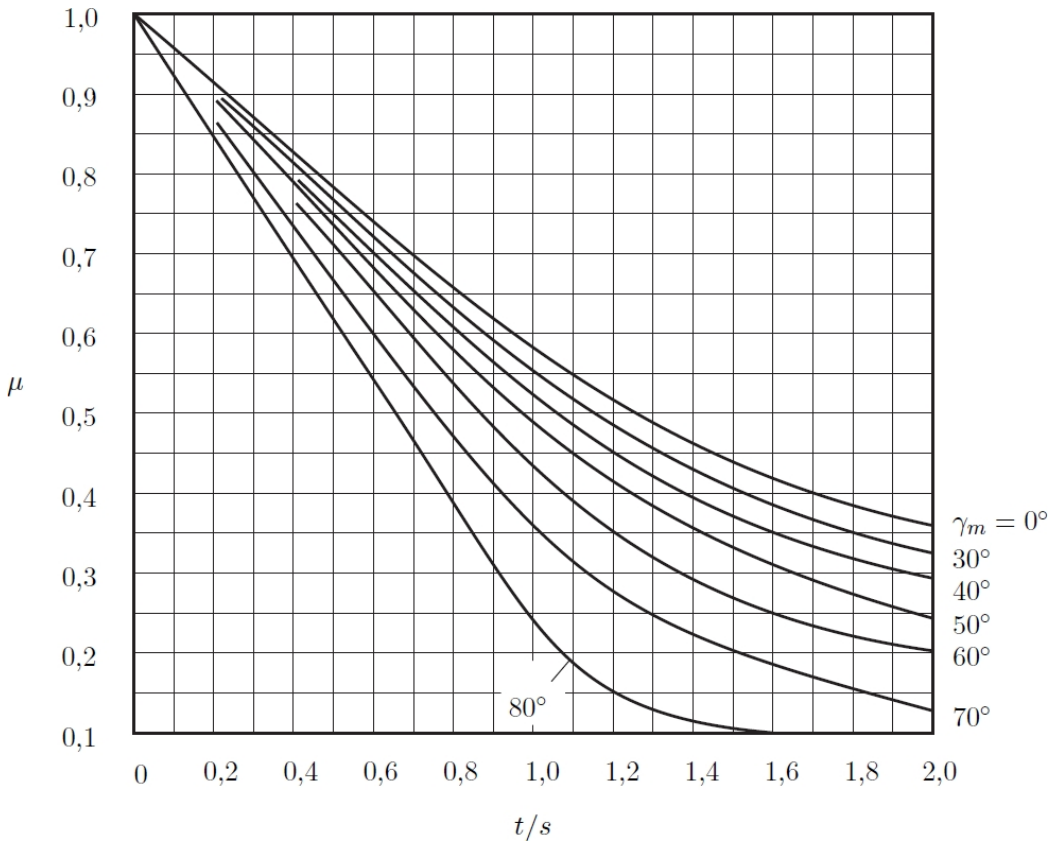

Fig. 6.4 Angular exaggeration factor for flow-free, infinitely thin, weakly curved circular arc grids [Jeschke 2017c].

Fig. 6.4. shows the angular overdrive factorμ with the aid of the already known variables, the mean flow angle and the split ratio.

The angular displacement due to curvature is defined as the difference between the flow angles and the metal angles:

$$\delta\alpha_w = \gamma_0 - \alpha_{50,i=0} \qquad (6.49)$$

$$\delta\alpha_w = \alpha_{51,i=0} - \gamma_1. \qquad (6.50)$$

The following also applies to the angular exaggeration factor:

$$\mu = \frac{\alpha_{50,i=0} - \alpha_{51,i=0}}{\gamma_{(0)} - \gamma_1}. \qquad (6.51)$$

If we then calculate the difference between the deflection angles of the blade and those of the flow, apply (6.45), divide by $(\gamma_E - \gamma_A)$ and apply (6.46), we obtain
an expression that is solved for $\delta\alpha_w$ looks like this:

$$\delta\alpha_w = \frac{1-\mu}{2\mu}(\alpha_{50,i=0} - \alpha_{51,i=0}). \qquad (6.52)$$

Since the angular exaggeration factor and the flow angles are known, it is now possible to calculate the angular exaggeration due to the influence of camber and, as a result, to calculate the blade design angles under the influence of camber:

$$\gamma_0 = \alpha_{50,i=0} + \delta\alpha_w \qquad (6.53)$$

$$\gamma_1 = \alpha_{51,i=0} - \delta\alpha_w . \qquad (6.54)$$

Since we cannot assume infinitely thin blades in reality, the previously calculated blade design angles must be adjusted with a correction value due to the finite profile thickness.

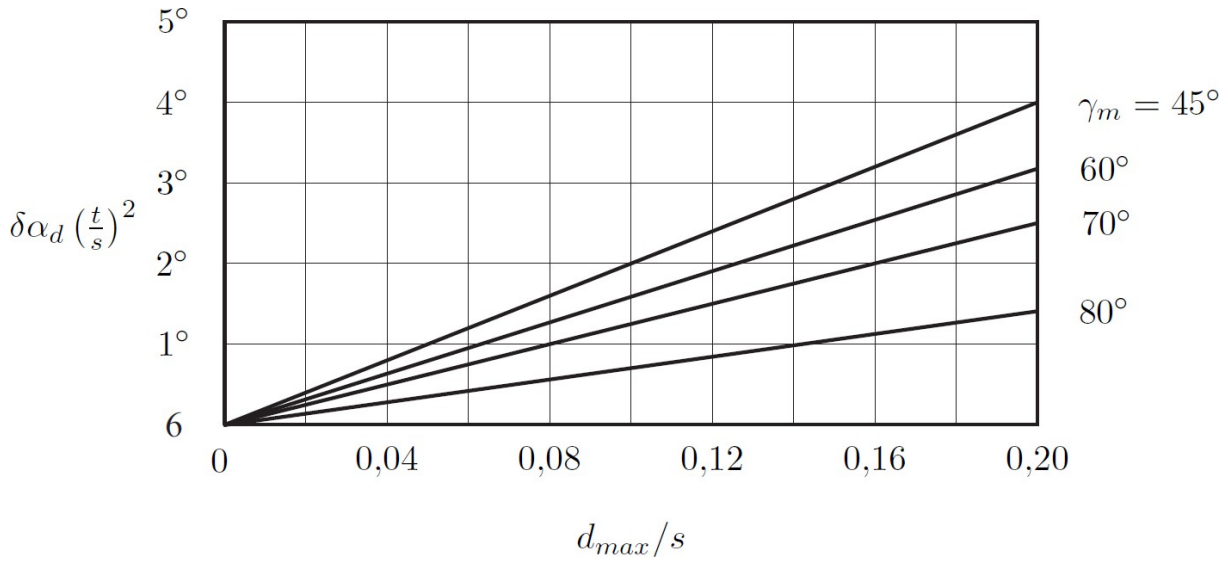

Fig. 6.5 Angular exaggeration due to the influence of the profile thickness with an incidence-free incident flow [Jeschke 2017c].

From Fig. 6.5. a value for $\delta\alpha_d \left(\frac{t}{s}\right)^2$ and then read off after $\delta\alpha_d$ be dissolved.

The principle of superposition can be used to offset the angular distortion due to the finite profile thickness and the profile curvature:

$$\gamma_0 = \alpha_{50,i=0} + \delta\alpha_w - \delta\alpha_d \qquad (6.55)$$

$$\gamma_1 = \alpha_{51,i=0} - \delta\alpha_w - \delta\alpha_d. \qquad (6.56)$$

The blade design angles of the rotor blade and guide vane can also be determined in the same way.

$\alpha_{(5.}$=0*deg*	$\alpha_{5.1}$=759 *deg*	$\frac{d_{max}}{s}$=1	$\frac{t}{s}$ =75
γ_m=380*deg*	μ= 0,66	$\Delta\alpha_w$= -0,*deg*	$\gamma_{0\,w}$=-0.*deg*
γ_{1w}=955	$\Delta\alpha_d$= 0,*deg*	γ_0= -0.*deg*	γ_1= 0.*deg*

Table 6.5 Results of the angular exaggeration of the stator

$\alpha'_{5.1}$ =841*deg*	$\alpha_{5.2}$=082 *deg*	$\frac{a_{max}}{s}$=1	$\frac{t}{s}$ =75
γ_m=767*deg*	μ= 0,58	$\Delta\alpha_w$= -0,*deg*	γ'_{1w} = 0,753 *deg*
γ_{2w}=170	$\Delta\alpha_d$= 0,*deg*	γ'_1= 0.691*deg*	γ_2= 1,*deg*

Table 6.6 Results of the angular exaggeration of the rotor

From the calculated angular exaggerations, the axial component of the chord length vector can now be used to calculate the radius and the center of a circular arc, which ensures the desired deflection. This was done using a CAD design program, which provides the following data

x_{Stator}=7*mm*	y_{Stator}=0*mm*	r_{Stator}=505*mm*
x_{Rotor}= -25, 003*mm*	y_{Rotor}= 0*mm*	r_{Rotor}= 39,233*mm*

Table 6.7 Arc radius and center point

A simple NACA 0010 profile was selected as the profile, as this a fairly large nose radius, which means that the profile does not react so sensitively to incorrect flow.

However, the thickness must be multiplied by a factor to arrive at our $\frac{dmax}{s}$ correspond. Furthermore, the thickness cannot simply be added to the Y component of the skeletal line, as this would distort the profile due to the circular arc. The added thickness is therefore calculated using the angle dependent on the pitch, which is calculated using an approximation

$$\alpha = \arctan\left(\frac{y_2 - y_1}{x_2 - x_1}\right). \qquad (6.57)$$

The corrected thickness difference then results from the thickness of the profile and the pitch angle:

$$\Delta d_{Profil} = \frac{d_{Profil}}{\cos(\alpha)} \qquad (6.58)$$

Furthermore, the skeletal line results from the formula of a circular arc:

$$y=\sqrt{-\overline{(x+x_{Stator})^2-r^2}}+c\,. \qquad (6.59)$$

Where by c in this case is only a factor freely chosen by us to integrate the profile into the respective configuration. Finally, the profile top and bottom pages can be calculated:

$$y_{Oberseite}=y+\Delta d_{Profil} \qquad (6.60)$$

$$y_{Unterseite}=y-\Delta d_{Profil} \qquad (6.61)$$

This results in the following two profiles for stator and rotor:

Stator	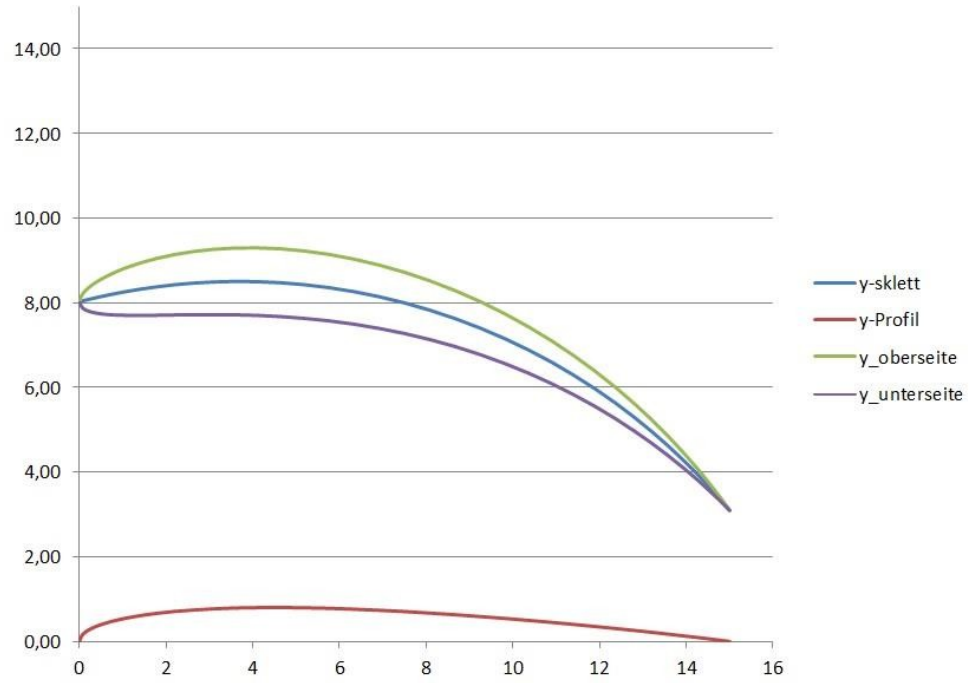

Rotor	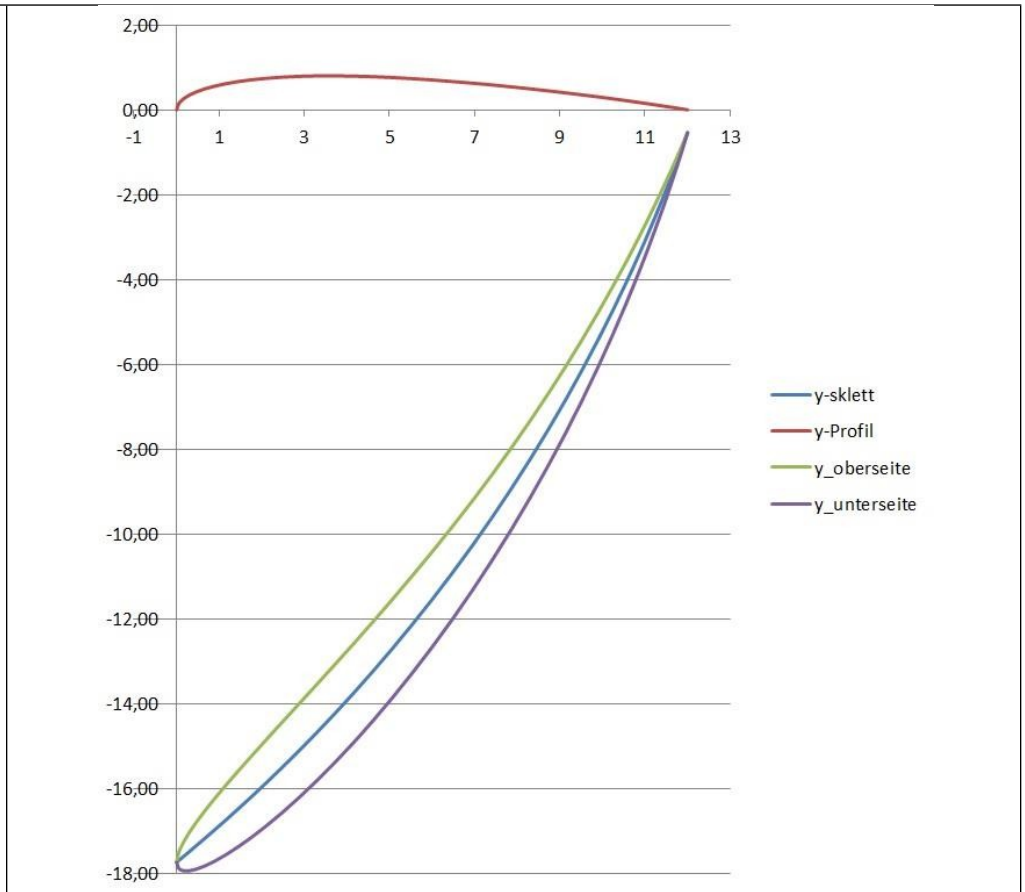

Table 6.6 Stator and rotor profile

7. Nozzle

7.1. Calculation Nozzle

A purely convergent nozzle is used to accelerate the gas after the turbine stage. The nozzle efficiency is estimated conservatively. The outlet state of the nozzle is declared here as plane 6. The pressure there corresponds to the ambient pressure. The following values are fixed or taken from previous calculations.

η_D=9	κ'=325	R'_L=287 $\frac{J}{kgK}$	c'_p=08 $\frac{J}{kgK}$
$p_{t5,2}$ = 149816, 8Pa	$T_{t5.2}$= 1110.K	p_0=Pa	

Table 7.1. initial values of the nozzle calculation

Using the values from Table 7.1, it is directly possible to calculate the exit velocity of the gas at the end of the turbine nozzle.

$$c_6 = \sqrt{2\eta_D \frac{\kappa'}{\kappa'-1} R'_L T_{t5,2} \left[1 - \left(\frac{p_0}{p_{t5,2}}\right)^{\frac{\kappa'-1}{\kappa'}}\right]} \qquad (7.1)$$

The calculated engine exit velocity is now used to convert the total temperature equation to the static temperature so that this can be calculated:

$$T_6 = Tt5_{.2} - \frac{c_6^2}{2 \cdot c'_p} \qquad (7.2)$$

The ideal gas law gives the density in state 6.

$$\rho_6 = \frac{p_{(0}}{R_L' T_6} \qquad (7.3)$$

The Mach number is also calculated from the total temperature and static temperature:

$$Ma_6 = \sqrt{\frac{2}{\kappa'-1}\left(\frac{T_{t5.2}}{T_6} - 1\right)}. \qquad (7.4)$$

To complete the calculations for the nozzle, the cross-sectional area and the diameter of the nozzle outlet are calculated:

$$A_6 = \frac{\dot{m}_{(5}}{\rho_6 c} \qquad (7.5)$$

$$D_6 = \sqrt{\frac{4A_6}{\pi}}. \qquad (7.6)$$

The values are as follows:

$c_6 = 462 \frac{m}{s}$	$T_6 = 1018,8K$	$\rho_6 = 347 \frac{kg}{m^3}$
$Ma_6 = 743$	$A_6 = 0.000917^{m(2)}$	$D_6 = 34.mm$

Table 7.2 Results of the nozzle calculation.

8. State diagrams and Shear calculation

The thrust is now calculated from the exit velocity and the mass flow of the engine using formula (2.52). As the thrust increases with higher exit velocities, it could theoretically be significantly increased by a thruster. However, this was deliberately omitted, as the focus should initially be on developing an operational engine without optimizing it down to the last detail.

$$F = \dot{m}_6 c_6 + A_6 (p_6 - p_0) - \dot{m}_0 c_0. \qquad (2.52)$$

As there is ambient pressure behind the turbine, $p_6 - p_0 = 0$. Furthermore, the engine should first be tested at standstill, which means that $c_0 = 0$ applies. This gives us

$$F = \dot{m}_6 c_6 = 67.86\ N \qquad (8.1)$$

This corresponds to a weight of 6.917 kg.

The following three diagrams illustrate the thermodynamic state variables that were calculated in the previous chapters.

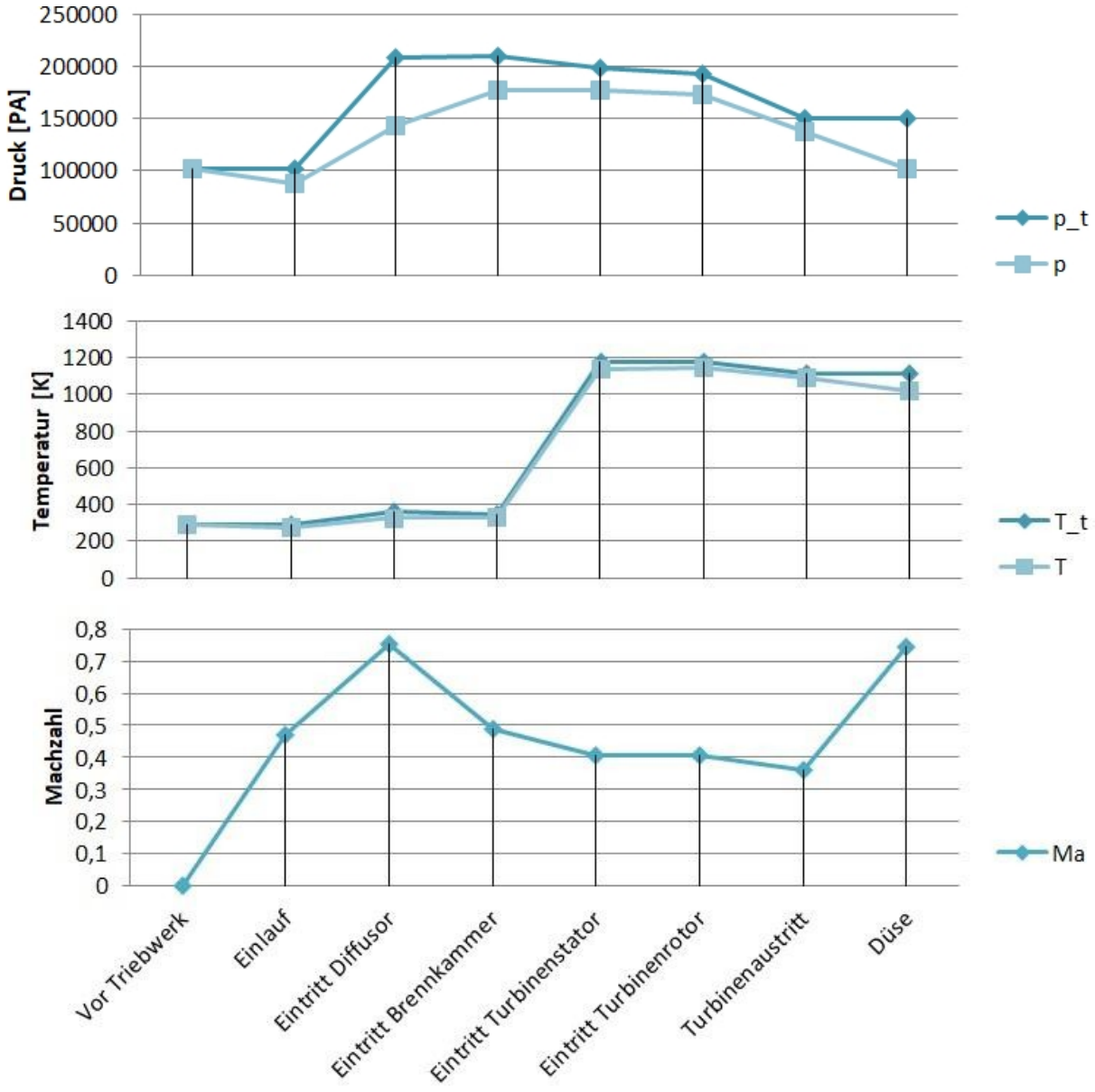

Fig. 7.1 Thermodynamic state variables in the engine levels

9. Summary and Outlook

This project has shown that it is possible to design a single-shaft jet engine in its basic dimensions on the basis of existing parts using relatively simple calculations and a one-dimensional approach, provided that a compressor with a corresponding characteristic map is available. This is particularly interesting because the fluid mechanical and thermodynamic relationships of a jet engine are generally very complex and are based on extensive derivations. By making simplifications and assumptions, it was possible to achieve good approximate results with relatively simple calculations.

The next step is to create CAD models of the parts to be manufactured. The components can then either be manufactured in-house or commissioned from external companies.
Furthermore, a test rig must be designed that offers the possibility of recording the following variables: Speed, pressure after the compressor or diffuser, engine inlet speed, fuel mass flow and the engine outlet temperature. Using these measured variables, it is possible to generate the engine or compressor map and compare it with the one created in advance.
If there are large deviations between these maps, it is possible to use the new maps to gradually improve and optimize the engine in the analogous way presented here.

10 Bibliography

Bräunling, Willy J. G.: Aircraft engines. Fundamentals of aero-thermodynamics, ideal and real cycle processes, thermal turbomachinery, components, emissions and systems. 3rd, fully revised and expanded ed. Springer, 2009 [Bräunling 2009]

Jeschke, Peter: Lecture reprint Fundamentals of turbomachinery. Institute for Jet Propulsion and Turbomachinery, RWTH Aachen University 2016 [Jeschke 2016a]

Jeschke, Peter: Lecture reprint Design of turbomachinery. Institute for Jet Propulsion and Turbomachinery, RWTH Aachen University, 2017 [Jeschke 2017a]

Jeschke, Peter: Lecture notes on aero engines I and II. Institute for Jet Propulsion and Turbomachinery, RWTH Aachen University, 2017 [Jeschke 2017b]

Jeschke, Peter; Broichhausen, Klaus; Grates, Daniel: Lecture Circulation Flow in Turbomachinery I and II. Institute for Jet Propulsion and Turbomachinery, RWTH Aachen University, 2017 [Jeschke 2017c]

Schröder, Wolfgang: Fluid mechanics. Aachener Beiträge zur Strömungsmechanik. 3rd corrected edition. Aerodynamic Institute and Chair of Fluid Mechanics, RWTH Aachen University, Wissenschaftsverlag Mainz, 2014 [Schröder 2014]

Wischnewski, Bernd: Calculation of the thermodynamic state variables of air, at: http://peacesoftware.de/einigewerte/luft.html (retrieved 20.09.2017). [Wischnewski 2017]

https://de.wikibooks.org/wiki/Tabellensammlung_Chemie/_spezifische_W%C3%A4rmekapazit%C3%A4ten (retrieved 02.11.2017). [8]

https://www.schweizer-fn.de/stroemung/druckverlust/druckverlust.php
Temperature dependence of c_p for gases (retrieved 22.12.2017). [9]

http://airfoiltools.com/
Airfool Plotter (retrieved 19.01.2018). [10]

http://www.uni-magdeburg.de/isut/LSS/Lehre/Arbeitsheft/VII.pdf Resistance laws of pipe flow (retrieved 22.12.2017). [11]

https://www.ingenieurkurse.de/stroemungslehre/hydrodynamik/reibungsbehaftete-stroemungen/berechnung-der-gesamten-verluste-in- Rohrleitungen/iterative-bestimmung-der- Rohrreibungszahl-lambda.html

Fluid mechanics (retrieved 22.12.2017) [12]